Anionic Polymerization and Block Copolymerization of *N,N*-Diethylacrylamide in the Presence of Triethylaluminum. Kinetic Investigation Using In-Line FT-NIR Spectroscopy

Xavier André,[†] Khaled Benmohamed, Alexander V. Yakimansky,[‡] Galina I. Litvinenko,[§] and Axel H. E. Müller*

Makromolekulare Chemie II and Bayreuther Zentrum für Kolloide und Grenzflächen, Universität Bayreuth, D-95440 Bayreuth, Germany

Received July 11, 2005; Revised Manuscript Received February 22, 2006

ABSTRACT: We present the first kinetic study of the anionic polymerization of a *N,N*-dialkylacrylamide, i.e., *N,N*-diethylacrylamide (DEAAm). The polymerization was initiated by ethyl α-lithioisobutyrate (EiBLi), poly(*tert*-butyl acrylate)-Li, and poly(*tert*-butyl methacrylate)-Li in the presence of triethylaluminum (Et_3Al) in tetrahydrofuran at −78 °C. In situ Fourier transform near-infrared (FT-NIR) fiberoptic spectroscopy was successfully used to follow the polymerization kinetics to elucidate its mechanism. The kinetics of this process are very complex. They involve two equilibria: activation of the monomer and deactivation of chain ends by Et_3Al. These two effects are in a delicate balance that depends on the ratio of the concentrations of Et_3Al, monomer, and chain ends. Polymers with narrow-molecular-weight distribution are produced, whereas broadly distributed polymer is obtained in the absence of Et_3Al. By using this method, well-defined poly(*N,N*-diethylacrylamide) (PDEAAm), poly(*tert*-butyl acrylate)-*block*-PDEAAm, and poly(*tert*-butyl methacrylate)-*block*-PDEAAm (co)-polymers were successfully synthesized, although the initiator or blocking efficiencies remained low ($f < 0.70$). The polymers obtained in the presence of Et_3Al are rich in heterotactic triads, whereas highly isotactic polymer is obtained in the absence of Et_3Al. In both cases, the polymers exhibit an lower critical solution temperature (LCST) with a cloud point at $T_c \approx 31$ °C in water.

Introduction

The interest in the living/controlled polymerization of mono- and dialkylacrylamides has been increasing due to their thermoresponsive properties in aqueous solution. Homopolymers of *N*-isopropylacrylamide (NIPAAm) and *N,N*-diethylacrylamide (DEAAm) exhibit a lower critical solution temperature (LCST) with a cloud point at ca. 32 °C, making these materials and their derivatives a very interesting class of polymers.[1,2]

The control of the stereostructure in anionic polymerization was described by early work on poly(*N,N*-dimethylacrylamide) (PDMAAm), synthesized using alkyllithium initiators. The polymers were reported to be highly crystalline and rich in isotactic (mm) triads.[3,4] Several groups have investigated the effect of counterions and temperature on the tacticity of the resulting polymer in the absence of additives. Xie and Hogen-Esch used different organometallic initiators in tetrahydrofuran (THF) at −78 °C in the absence of additives.[5] Only large counterions such as cesium gave homogeneous reaction mixtures, leading to narrowly distributed polymers. Neither transfer nor terminations were observed, and the experimental number-average molecular weights, M_n, were in accordance with calculated ones. The living character was lost when the polymerization was carried out at 0 °C. Under the same conditions, *N,N*-dimethylmethacrylamide did not polymerize, presumably due to an insufficient stabilization of the propagating amidoenolate. Kobayashi et al. observed a heterogeneous polymerization of DMAAm and DEAAm by using organolithium initiator in the presence of LiCl, leading to broadly distributed polymers (PDI > 3).[6] Nakhmanovich et al. polymerized DMAAm with several initiators containing alkaline earth metal compounds (Mg, Ca, Ba), and they reported the influence of the counterion size on the tacticity but no evidence on the living character.[7] Freitag et al. reported the polymerization of DEAAm via anionic and group transfer polymerization (GTP) methods and reported the influence of the tacticity on the measured cloud point, T_c.[8,9] In comparison to the value of T_c = 32 °C claimed for PDEAAm synthesized via free-radical polymerization (atactic polymer), a value of 30 °C was observed for predominantly syndiotactic polymers synthesized via GTP, whereas a value of 36 °C was measured for predominantly isotactic polymers synthesized via anionic polymerization using butyllithium as initiator without additive.

Major advances were reported by Nakahama et al. for the anionic polymerization of DMAAm and DEAAm by the use of organolithium and organopotassium initiators in the presence of Lewis acids (Et_2Zn, Et_3B).[6,10,11] The great influence of the system initiator/additive/solvent on the tacticity and the solubility of the resulting polymer was clearly demonstrated. The authors suggested that the coordination of the amidoenolate with the Lewis acid leads to a change of the stereostructure of the final polymer along with the retardation of the polymerization. Highly isotactic PDEAAm was obtained by using LiCl with an organolithium initiator, whereas highly syndiotactic and atactic polymers were obtained in the presence of Et_2Zn and Et_3B, respectively. Indeed, the polymers produced in the presence of Et_3B show a very broad distribution of the carbonyl carbon resonance, and their degree of syndiotacticity increases with the ratio B/Li, but it does not reach as high a level as that

* To whom correspondence should be addressed. E-mail: axel.mueller@uni-bayreuth.de.

[†] Present address: Cornell University, Materials Science & Engineering Department, Ithaca, NY 14853.

[‡] Permanent address: Institute of Macromolecular Compounds of the Russian Academy of Sciences, Bolshoi prospect 31, 199004 St. Petersburg, Russia.

[§] Permanent address: Karpov Institute of Physical Chemistry, Vorontsovo pole 10, 105064 Moscow, Russia.

10.1021/ma051506a CCC: $33.50
Published on Web 03/28/2006

observed with Et_2Zn. Polymers rich in syndiotactic triads were not soluble in water, whereas other microstructures lead to hydrophilic polymers.[11] Ishizone et al. also reported the use of Lewis acids (Et_2Zn, Et_3B) for the controlled polymerization of *tert*-butyl acrylate initiated by organocesium compounds in THF.[12,13] They reported the successful synthesis of poly(*tert*-butyl acrylate)-*block*-poly(*N*,*N*-diethylacrylamide) in THF at −78 °C. For that purpose, *tert*-butyl acrylate was first initiated by an organocesium initiator (Ph_2CHCs) in the presence of Me_2Zn, and DEAAm was then initiated by the poly(*tert*-butyl acrylate)-Cs macroinitiator, leading to a well-defined block copolymer ($M_w/M_n = 1.17$).[12]

Only one example was reported recently by Kitayama et al. for the polymerization of DMAAm in toluene. Living character was observed by using a system based on *tert*-butyllithium/bis(2,6-di-*tert*-butylphenoxy)ethylaluminum in toluene at 0 °C.[14] Well-defined block copolymers PDMAAm-*block*-poly(methyl methacrylate) could be obtained in good yield, but no kinetic studies were performed. Using ^{13}C NMR spectroscopy, the authors observed the preferential coordination of $EtAl(ODBP)_2$ to the carbonyl group of DMAAm and suggested an activated monomer mechanism where the adduct R_3Al·DMAAm propagates first until complete conversion followed by the polymerization of activated methyl methacrylate (R_3Al·MMA). Aluminum alkyl derivatives were also introduced for the polymerization of alkyl (meth)acrylates in toluene.[15−18] Living and stereospecific polymerizations were observed using *tert*-butyllithium/*bis*(2,6-di-*tert*-butylphenoxy)methylaluminum[19,20] and *sec*-butyllithium/diisobutyl(2,6-di-*tert*-butyl-4-methylphenoxy)aluminum.[21] Living/controlled polymerizations of alkyl (meth)acrylates were also reported using simple trialkylaluminum compounds in the presence of Lewis bases (12-crown-4, methyl pivalate, methyl benzoate, and *N*,*N*,*N*′,*N*′-tetramethylenediamine)[22−27] or tetraalkylammonium salts.[22,28] Recently, the use of triisobutylaluminum in combination with potassium *tert*-butoxide was successfully reported for the living anionic polymerization of *tert*-butyl acrylate (*t*BA) and methyl methacrylate (MMA) in toluene at 0 °C.[29,30]

Because of their acidic proton, the direct anionic polymerization of *N*-monoalkylacrylamides such as NIPAAm is not possible. By using *N*-methoxymethyl-substituted NIPAAm, well-defined polymers were synthesized using an organopotassium initiator in the presence of Et_2Zn, but no living character was described.[31] The use of *N*-trimethylsilyl-substituted NIPAAm leads to highly isotactic polymers, but no molecular weight distributions were shown due to the poor solubility of the resulting polymers in common solvents.[32] However, these promising methods have opened new synthetic strategies to polymerize *N*-monosubstituted acrylamide monomers with the advantages of anionic polymerization.

By using controlled radical polymerization (CRP) processes, well-defined PNIPAAm and PDMAAm have been synthesized recently. Reversible addition fragmentation transfer (RAFT),[33−35] atom transfer radical polymerization (ATRP),[36,37] and nitroxide mediated radical polymerization (NMRP)[38,39] were used. More recently, several groups reported the control of tacticity by CRP in the presence of yttrium- and ytterbium-based Lewis acid for NIPAAm via RAFT[40,41] and for DMAAm via RAFT and ATRP.[42] Nevertheless, anionic polymerization remains the best synthetic way to obtain well-defined (co)polymers up to complete monomer conversion, high molecular weight, and with desired microstructure.

To our knowledge, no kinetic investigations of the anionic polymerization of alkylacrylamides have been published so far. Besides the interesting properties of PDEAAm in aqueous solution, the monomer DEAAm is an ideal compound for Fourier transform near-infrared (FT-NIR) measurements, as it shows a distinct overtone of the vinylic C−H stretching at ca. 6156 cm^{-1}.[43] The variation of the peak height at this wavenumber can be followed throughout the reaction until the peak disappears at complete monomer conversion.

Herein, we report kinetic studies of the anionic polymerization of DEAAm in THF at −78 °C. Ethyl α-lithioisobutyrate (EiBLi), poly(*tert*-butyl methacrylate)-Li, and poly(*tert*-butyl acrylate)-Li (P*t*BMA-Li, P*t*BA-Li) were used as (macro)-initiators in the presence of Et_3Al. The influence of the reaction parameters ($[DEAAm]_0$, $[Initiator]_0$, $[Et_3Al]_0$) are investigated independently to propose a polymerization mechanism. The influence of the additive on the tacticity and solubility of the resulting polymers is also discussed.

Being a Lewis acid, Et_3Al might coordinate with all the Lewis bases present in the reaction medium. Amidoenolate chain ends, monomer, and polymer carbonyl groups as well as THF compete for coordination with Et_3Al. The possible interactions are shown in Scheme 1, together with the energy gains calculated by density functional theory (DFT).[44] The calculations on the trimeric model compound, i.e., an amidoenolate having two penultimate units, showed a strong tendency to coordinate with Et_3Al (stronger than the binding of Et_3Al to THF), this tendency being dependent on the tacticity of the chain end ($\Delta E = -9$ to -24 kJ·mol^{-1}). The tendency of noncoordinated chain ends to aggregate to dimers is very weak and also depends on the tacticity (Scheme 2); the dimers are regarded to be much less reactive than unimers or even inactive (dormant). Previous kinetic and quantum-chemistry investigations on aluminum alkyl−esterenolate complexes in nonpolar solvent also indicated the existence of an ester enol aluminate and a less-reactive dimeric associate.[22,28,45]

The DFT calculations also indicate the coordination of Et_3Al with the carbonyl group of DMAAm; however, this bond is not as strong as that of the chain end ($\Delta E = -7$ kJ·moL^{-1}). It may indicate that free monomer and activated monomer are in equilibrium. Binding of Et_3Al to the carbonyl groups of the polymer is calculated to be less favorable than the other coordination modes ($\Delta E = +8$ kJ·mol^{-1} for *mm* triads, -10 kJ·mol^{-1} for *rr* triads, and -1 kJ·mol^{-1} for *mr* triads). Because the resulting polymers are mainly heterotactic, we assume that $\Delta E \cong 0$. The effect of Et_3Al on the microstructure of the final polymer is discussed further below.

Experimental Section

Materials. Tetrahydrofuran (THF, Merck) was purified by refluxing over CaH_2 and distilled from potassium before use. Triethylaluminum (Et_3Al, Aldrich, 1 M in hexane) was used as received. The monomers *tert*-butyl methacrylate, and *tert*-butyl acrylate (*t*BMA, *t*BA, BASF) were three times degassed under high vacuum (10^{-5} mbar), and Et_3Al was added dropwise until a yellowish color appeared. The mixture was stirred and condensed into an ampule and stored under dry nitrogen atmosphere. DEAAm was synthesized by the reaction at $T < 10$ °C in toluene (Merck) of a 2-fold excess of diethylamine and acryloyl chloride (96%, Aldrich). The crude DEAAm was then purified five times from CaH_2 by fractional distillation under reduced pressure, and it was three times degassed prior to the polymerization. Ethyl α-lithioisobutyrate (EiBLi) was synthesized according to the method of Lochmann and Lim.[46] Diphenylhexyl-lithium (DPHLi) was prepared by the reaction of *n*-butyllithium (*n*-BuLi, Acros, 1.3 M in cyclohexane/hexane, 92:8) and 1,1-diphenylethylene (DPE, 97%, Aldrich, freshly distilled over *n*-BuLi) in situ ([DPE]/[*n*-BuLi] = 1.1). LiCl (Fluka, anhydrous ≥98%) was dried in high vacuum at 300 °C for 3 days and dissolved in dry THF.

Scheme 1. Competing Interactions of Et_3Al and DFT-Ccalculated Energy Differences[44]

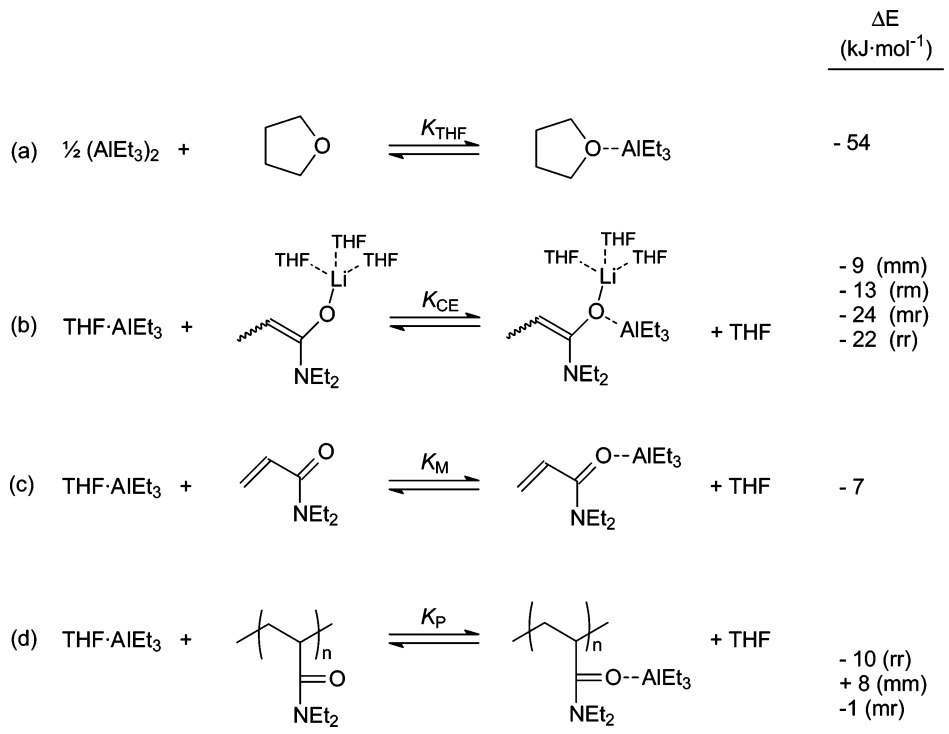

Scheme 2. Aggregation of the Amidoenolate Chain Ends in the Absence of Et_3Al

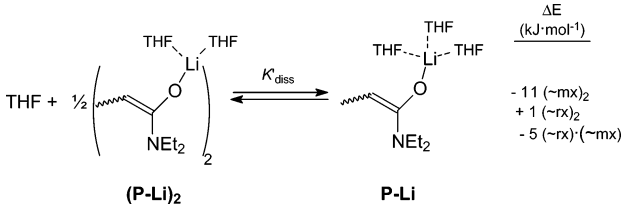

Equipment and In-Line FT-NIR Spectroscopy. The sequential anionic polymerizations were performed under dry nitrogen pressure in a thermostated glass reactor (Büchi) equipped with an all-glass immersion transmission probe (Hellma) with an optical path length of 10 mm connected via fiberoptics to a Nicolet Magna 560 FT-IR spectrometer equipped with a white light source and a PbS detector.[47] Data processing of NIR spectra was performed with Nicolet's OMNIC Series software version 5.2. Each spectrum was constructed with 16 scans with a resolution of 8 cm^{-1} and recorded every 3.7 s. Prior to the measurement, a blank spectrum of the solution containing the initiator, and eventually the additive, was recorded in the absence of a monomer at the working temperature. The measurement was started before injection of the first monomer. The baseline for signal height determination was drawn from 7000 to 6300 cm^{-1}, and the FT-NIR spectra of DEAAm were obtained after solvent subtraction to yield a pure component spectrum and to determine conversions because THF has strong absorptions close to the overtone vibrations of DEAAm. For the block copolymerization, *t*BMA and *t*BA polymerizations kinetics (precursors) were monitored using the same procedure.

Homopolymerization of DEAAm. The reactor containing ca. 600 mL of dry THF was cooled to −78 °C. The appropriate amount of Et_3Al was injected to the reactor via a syringe (12.0 mmoL; 18.8 mmol·L^{-1}, run C). The initiator, EiBLi (49.4 mg, 0.63 mmol·L^{-1}) was dissolved in 10 mL of dry toluene in a Rotaflo-sealed ampule and introduced into the reactor. Polymerization was started after stabilization of the temperature at $T = -78$ °C by injection of DEAAm (28.6 mmol; 44.9 mmol·L^{-1}) via a syringe ($t = 0$). A degassed solution of methanol/acetic acid (9:1 v/v) was used as a quenching agent. Experiments varying the inititial concentrations of EiBLi and Et_3Al were performed using the same procedure at $T = -78$ °C.

Block Copolymerization. As shown in Scheme 3, the initiator (DPHLi, 1.1 mmol; 1.8 mmol·L^{-1}, run L) was formed by the reaction of DPE and *n*-BuLi in the THF solution of LiCl at −30 °C (11.8 mmol; 18.5 mmol·L^{-1}). The monomer *t*BMA (55.4 mmol; 87.0 mmol·L^{-1}) was injected via a syringe into the reactor to start the polymerization of the precursor. The characteristic red color of the DPHLi initiator disappeared instantaneously. After full conversion of *t*BMA, the temperature was cooled to −78 °C (ca. 1 h), and then Et_3Al (8 mmol; 12.6 mmol·L^{-1}) and DEAAm (57.2 mmol; 89.9 mmol·L^{-1}) ($t = 0$) were added successively. A degassed solution of methanol/acetic acid (9:1 v/v) was used as a quenching agent. An aliquot of the final solution was taken and dried for 2 days under vacuum to result in the crude copolymer. The rest of the copolymer was recovered by precipitation into a large excess of *n*-hexane, filtered and dried for 2 days under vacuum. This process removes unreacted P*t*BMA precursor, leading to the purified copolymer. Traces of LiCl were removed from P*t*BMA precursor by 1 day of stirring in benzene followed by a filtration. The clear solutions were freeze-dried from benzene. Experiments with varying the initial concentrations of DEAAm were performed using the same procedure at −78 °C. The synthesis and purification of P*t*BA-*b*-PDEAAm copolymer were carried out using the same experimental conditions, except that both monomers *tert*-butyl acrylate (*t*BA) and DEAAm were polymerized at the same temperature (−78 °C).

Characterization of Polymers. Polymers were characterized by size exclusion Chromatography (SEC) using a Waters 510 HPLC Pump, a Bischoff 8110 RI detector, a Waters 486 UV detector ($\lambda = 270$ nm), and a 0.05 M solution of LiBr in 2-*N*-methylpyrrolidone (NMP) as eluent. PSS GRAM columns (300 mm × 8 mm, 7 μm): 10^3, 10^2 Å (PSS, Mainz, Germany) were thermostated at 70 °C. A 0.4 wt % (20 μL) polymer solution was injected at an elution rate of 1 mL·min^{-1}. Polystyrene standards were used to calibrate the columns, and methyl benzoate was used as an internal standard. A second SEC setup was performed in pure THF at an elution rate of 1 mL·min^{-1} using a Shodex RI-101 detector, a Waters 996 photodiode array detector (PDA), and PSS SDVgel columns (300 mm × 8 mm, 5 μm): 10^5, 10^4, 10^3, and 10^2 Å. Poly(*tert*-butyl methacrylate) standards were used to calibrate the columns. MALDI-TOF mass spectrometry was performed on a Bruker Reflex III equipped with a 337 nm N_2 laser and 20 kV acceleration voltage. Dihydroxybenzoic acid (DHB) or dithranol were used as matrix. Samples were prepared from dimethylacetamide solution by mixing

Scheme 3. Anionic Polymerization of *N,N*-Diethylacrylamide Initiated by a Poly[*tert*-butyl (meth)acrylate]-Li Macroinitiator in the Presence of Et_3Al.

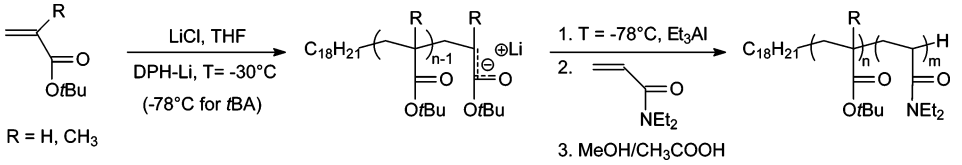

Table 1. Anionic Polymerization of DEAAm Initiated by Ethyl α-Lithioisobutyrate (EiBLi) in the Presence of Et_3Al in THF at −78 °C[a]

run	$[EiBLi]_0$ mmol·L^{-1}	$[Et_3Al]_0$ mmol·L^{-1}	$r = [Et_3Al]_0/[I]_0$	$10^{-3}\cdot M_{n,theo}$[b]	$10^{-3}\cdot M_{n,exp}$[c] (MALDI)	$10^{-3}\cdot M_{n,exp}$[d] (SEC)	M_w/M_n[d] (SEC)	f[e]
A	0.87	0	0	6.8	16.5[f]	12.1	2.13	0.41
B	0.65	4.7	7.2	8.8	26.0	17.6	1.03	0.34
C	0.63	18.8	29.8	9.1	39.4	30.8	1.05	0.23
D	0.74	30.8	41.6	7.7	39.2[f]	28.7	1.10	0.20
E	1.14	19.0	16.7	5.2	22.4	14.0	1.06	0.23
F	1.69	18.8	11.1	3.5	7.2	5.1	1.05	0.49

[a] Full conversions observed in all cases, $X_p = 1$, $[M]_0 = [DEAAm]_0 = 44.1-45.4$ mmol·L^{-1}. [b] $M_{n,theo,} = X_p\cdot[M]_0/[I]_0\cdot M_{DEAAm} + M_{initiator}$. [c] After precipitation in *n*-hexane, linear mode. [d] After precipitation in *n*-hexane, PS calibration. [e] Initiator efficiency, $f = M_{n,\,theo}/M_{n,MALDI}$. [f] Using eq 1.

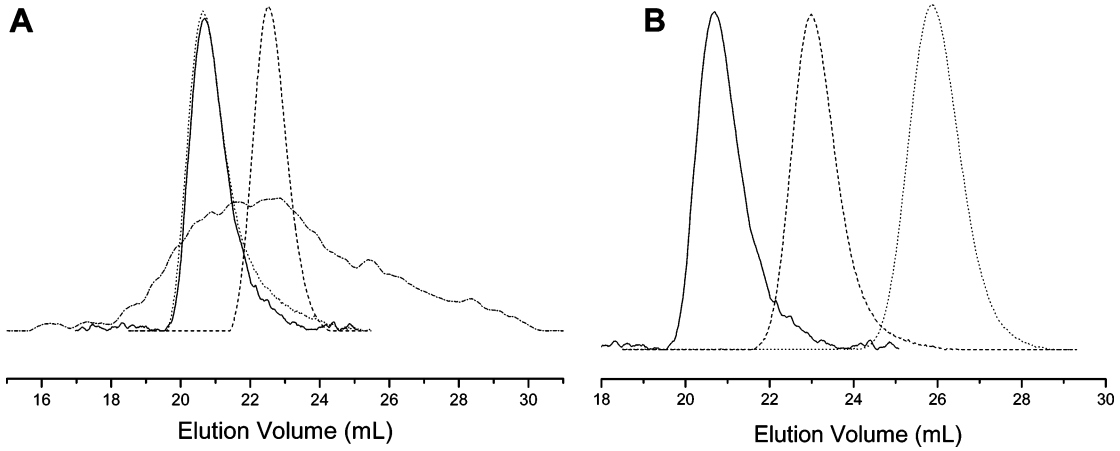

Figure 1. (A) SEC traces of the PDEAAm obtained with EiBLi/Et_3Al in THF at −78 °C by varying $[Et_3Al]_0$: (—·—) 0, (- - -) 4.7, (···) 18.8, and (—) 30.8 mmol·L^{-1}. (B) Variation of the initial initiator concentration, $[EiBLi]_0$: (—) 0.63, (- - -) 1.14, and (···) 1.69 mmol·L^{-1}. Experimental conditions: see Table 1.

matrix (10 g·L^{-1}) and sample (10 g·L^{-1}) in a ratio 10:1. No additional salt was needed for the measurement. The number-average molecular weights, M_n, were determined in the linear mode. The MALDI measurements were reproducible in the range of ±3%. ^1H and ^{13}C NMR spectra were recorded on a Bruker AC-250 spectrometer in THF-d_8 or $CDCl_3$ at room temperature. To ensure a good resolution of the ^{13}C NMR spectra for the determination of the polymer microstructure, 13 000 scans were accumulated.

Results and Discussion

1. Polymerization of DEAAm. (i) Initiation with EiBLi. A series of PDEAAm were synthesized using ethyl α-lithioisobutyrate (EiBLi) as an initiator in the presence and absence of Et_3Al in THF at −78 °C (Table 1). EiBLi is known as a unimeric model of the poly(alkyl methacrylate) living chains and was used as an initiator in numerous kinetic studies on alkyl acrylates and alkyl methacrylates.[28,48,49] PDEAAm synthesized in the absence or in the presence of Et_3Al were obtained in quantitative yield, and the polymerization media were clear and transparent up to 100% monomer conversion. Polymer produced in the absence of Et_3Al showed a broad molecular weight distribution ($M_w/M_n = 2.1$), whereas in the presence of Et_3Al, well-defined polymers were obtained ($M_w/M_n \leq 1.10$). Figure 1 shows the SEC traces of PDEAAm obtained at various Et_3Al and EiBLi initial concentrations. The SEC characterization of polymers bearing an amide function like PNIPAAm in THF involves various problems[50] due to chain aggregation after complete drying of the polymer samples and adsorption on the columns.[51] To circumvent this problem, the addition of salt (Bu_4NBr)[52] or triethylamine/methanol to THF was proposed.[53] Furthermore, because of their stereoregular structure, PDEAAm or PNIPAAm produced by anionic polymerization are poorly soluble in common solvents, and their characterization is commonly performed in *N,N*-dimethylformamide (DMF) or in *N,N*-dimethylacetamide (DMAc).[11,31] We have obtained good results by using 2-*N*-methylpyrrolidinone (NMP) with LiBr (0.05 M) as an eluent in combination with polar PSS GRAM columns thermostated at 70 °C. As the columns were calibrated against linear polystyrene standards, the molecular weight of each narrowly distributed PDEAAm sample was measured additionally by MALDI-TOF mass spectrometry.

Figure 2 shows the MALDI-TOF mass spectrum of a PDEAAm of lower molecular weight (run F), measured without any added salt. The spectrum (Figure 2A) shows a second peak of lower intensity at ca. $m/z = 3500$, which is attributed to doubly charged chains that are often observed for polar polymers ($z = 2$).[54] Thus, a multipeak Gaussian fitting procedure was used to calculate the molecular weights. The expanded spectrum from 6000 to 6300 Da is shown in Figure 2C, and the series of observed masses are in good agreement with the expected chain structure $[C_6H_{11}O_2 + DP_n\cdot(C_7H_{13}NO)]$ with a repeat unit of 127.09 Da = monoisotopic mass (average mass = 127.19) corresponding to one DEAAm unit and a residual fragment of

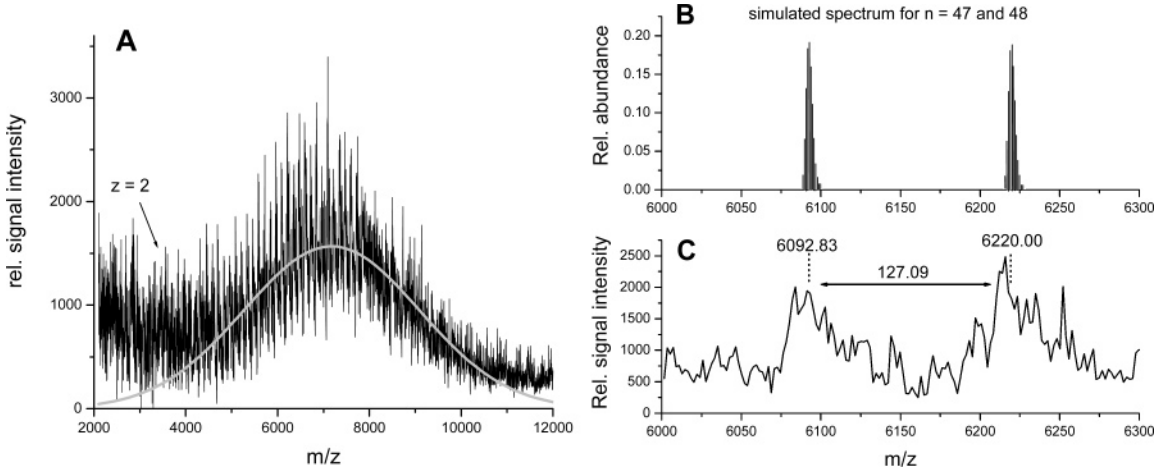

Figure 2. MALDI-TOF mass spectrum of PDEAAm (run F). (A) Complete spectrum measured without salt in the linear mode. The gray line corresponds to a multipeak Gaussian fit. (B) Simulated peak distribution due to isotopic abundance. (C) Expanded experimental spectrum.

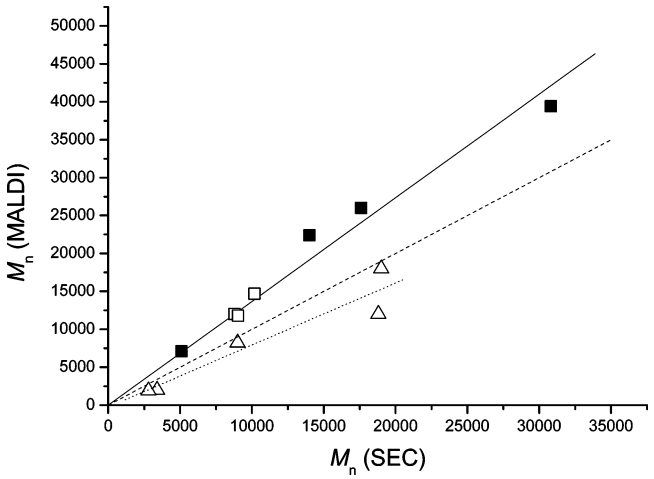

Figure 3. Plot of M_n (MALDI) vs M_n (SEC), SEC in NMP for PDEAAm obtained with (■) EiBLi/Et_3Al, and (□) DPHLi/Et_3Al in THF at −78 °C. (—) Linear fit of data points; (- - -) line expected for M_n (MALDI) = M_n (SEC). For comparison, well-defined PNIPAAm[55] are shown (···△···). The characterization of PDEAAm obtained with DPHLi/Et_3Al is shown in the Supporting Information, Table S2.

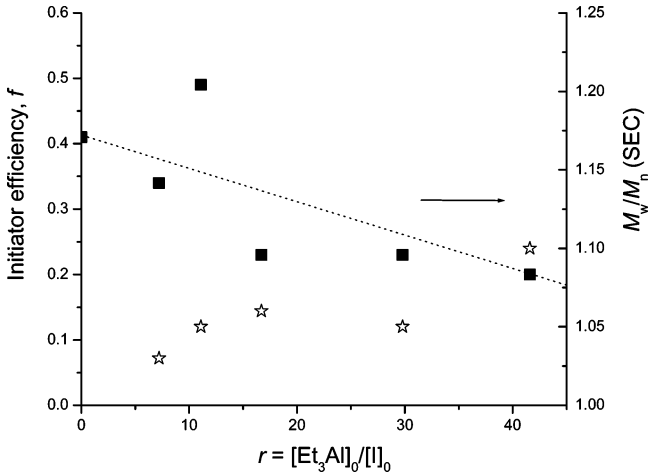

Figure 4. Dependence of the initiator efficiency, f (■), and the polydispersity index, M_w/M_n (☆) on the ratio $r = [Et_3Al]_0/[I]_0$ synthesized using EiBLi in the presence of Et_3Al in THF at −78 °C. Experimental conditions: see Table 1.

115.08 Da monosiotopic mass (average mass = 115.15 Da) corresponding to the initiator fragment.

The number-average molecular weights, M_n, determined by SEC using a PS calibration underestimate the real molecular weights (Table 1, Figure 3). A linear fit of the plot of M_n (MALDI) vs M_n (SEC) for the PDEAAm samples obtained with organolithium initiators in the presence of Et_3Al results in the relation,

$$M_n\,(\text{MALDI}) = (1.40 \pm 0.05)\cdot M_n\,(\text{SEC}) \qquad (1)$$

It was reported by Ganachaud et al. and by Schilli et al. that the SEC evaluation of linear PNIPAAm in pure THF and in THF + tetrabutylammonium bromide (Bu_4NBr), respectively, gives significantly higher molecular weights than those obtained from MALDI-TOF analysis.[35,51] These atactic polymers were obtained via RAFT polymerization. The characterization of well-defined linear PNIPAAm obtained by RAFT using benzyl 1-pyrrolecarbodithioate as a chain transfer agent[55] are also plotted in Figure 3. Their absolute molecular weights are slightly overestimated in NMP but not as much as it was reported by Schilli et al. in THF + salt. Even if the direct comparison of PNIPAAm and PDEAAm is not possible, this observation may be attributed to the intrinsic difference of the chemical structure of both polymers. As a monoalkylacrylamide, PNIPAAm may form hydrogen bonds with NMP. In contrast, PDEAAm does not bear an amide proton, and hydrogen bonding is not possible. Thus, for a given absolute molecular weight, the hydrodynamic volume in NMP of a PDEAAm coil is smaller than that of PNIPAAm, and it therefore shows an apparently lower M_n. PDEAAm synthesized via anionic polymerization is rich in heterotactic triads (see below) and, therefore, should have a microstructure comparable to PNIPAAm.

Relatively low initiator efficiencies, $0.23 \le f \le 0.49$, are calculated from the M_n obtained by MALDI-TOF MS. With increasing ratio $r = [Et_3Al]_0/[I]_0$, f decreases, as suggested in Figure 4, reaching a plateau at $f \approx 0.20$ for $r \ge 10$. The effect of Et_3Al on polymerization rates will be discussed in detail below.

A few attempts were carried out using DPHLi as an initiator in the presence of Et_3Al. Narrowly distributed polymers were obtained at −78 °C (M_w/M_n = 1.15−1.19), while broad molecular weight distributions (MWD) were observed at 0 °C (M_w/M_n > 1.7). For details, see Table S2 in the Supporting Information. However, the living polymers were unable to initiate the polymerization of *tert*-butyl acrylate (*t*BA) or *tert*-butyl methacrylate (*t*BMA). This was attributed to the coordination of Et_3Al to the amidoenolate active chain, which decreases the nucleophilicity of the resulting ate-complex.

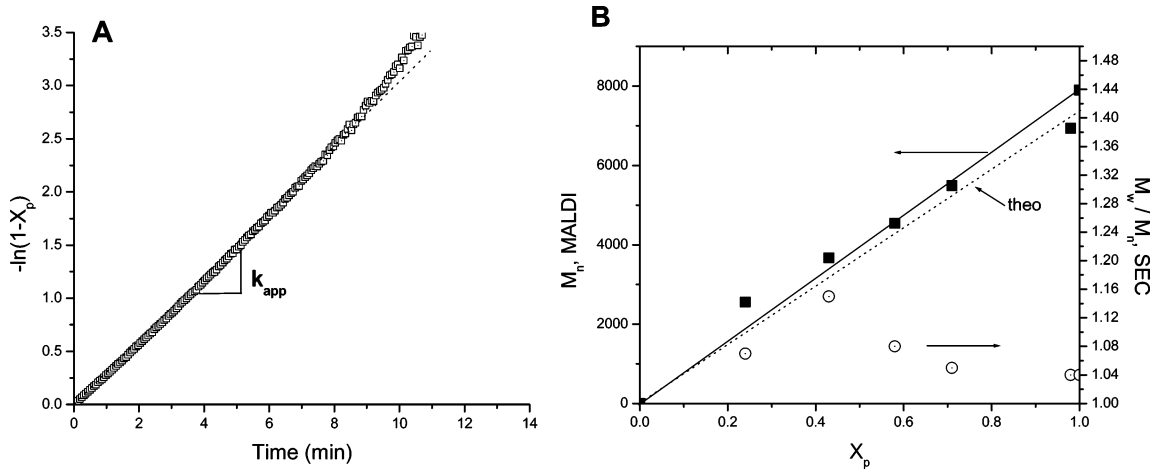

Figure 5. (A) First-order time-conversion plot for the polymerization of *t*BMA initiated by DPHLi/LiCl in THF at −30 °C, run J. (B) Corresponding dependence of M_n (MALDI) (■), and of the polydispersity index, M_w/M_n (SEC) (○), on *t*BMA conversion, X_p. Experimental conditions: $[t\text{BMA}]_0 = 86.4$ mmol·L^{-1}, $[\text{DPHLi}]_0 = 1.74$ mmol·L^{-1}, $[\text{LiCl}]/(f\cdot[\text{DPHLi}]_0) = 11.3$.

Table 2. Anionic Polymerization of DEAAm Initiated by a Poly(*tert*-butyl acrylate)-Li and Poly(*tert*-butyl methacrylate)-Li [P*t*B(M)A-Li] Macroinitiators in the Presence of Et_3Al and LiCl in THF at −78 °C[a,b]

run	initiator	$[I]_0$[c] mmol·L^{-1}	$[\text{DEAAm}]_0$ mmol·L^{-1}	$[Et_3Al]_0$ mmol·L^{-1}	$r = [Et_3Al]_0/[I]_0$	$r^* = [Et_3Al]_0/[P^*]_0$[d]	$10^{-3}\cdot M_{n,theo}$[e]	$10^{-3}\cdot M_{n,exp}$[f] (MALDI)	f[g]	$10^{-3}\cdot M_{n,exp}$[h] (SEC)	M_w/M_n[h] (SEC)
G	P*t*BA-Li	1.77	94.0	12.9	7.30	48.6	12.7	51.8	0.15	28.5	1.12
H	P*t*BA-Li	2.35	137	13.9	5.90	23.7	11.4	45.2	0.25	29.7	1.08
I	P*t*BA-Li	0.55	92.0	3.2	5.80	18.8	24.3[i]	77.6	0.31	48.9	1.09
J	P*t*BMA-Li	1.62	11.2	12.5	7.72	11.0	8.8	11.5	0.70	9.3	1.05
K	P*t*BMA-Li	1.71	44.7	12.5	7.31	18.3	10.8	16.0	0.40	11.7	1.05
L	P*t*BMA-Li	1.51	89.9	12.6	8.34	15.7	16.1	22.7	0.53	18.1	1.06
M	P*t*BMA-Li	1.38	202	12.6	9.13	21.7	27.9	79.0	0.42	57.4	1.04

[a] Full conversions observed in all cases, $X_p = 1$,from FT-NIR data. [b] *t*BA and *t*BMA were polymerized by DPHLi/LiCl at −78, and −30 °C, respectively, $[\text{LiCl}]/[\text{DPHLi}]_0 = 7.10-15.9$. [c] Effective macroinitiator concentration, see Table S1 in the Supporting Information. [d] $[P^*]_0$, active chain-end concentration, calculated using the blocking efficiency, *f*. [e] $M_{n,theo} = X_p \cdot [M]_0/[I]_0 \cdot M_{DEAAm} + M_{precursor}$. [f] After precipitation in *n*-hexane, linear mode. [g] Blocking efficiency, $f = (M_{n,theo} - M_{n,prec})/(M_{n,exp} - M_{n,prec})$. [h] After precipitation in *n*-hexane, PS calibration. [i] $X_p = 0.88$.

(ii) Initiation by Poly[*tert*-butyl (meth)acryloyl]-Li/LiCl. *tert*-Butyl methacrylate (*t*BMA) was polymerized in a living way using the system DPHLi/LiCl in THF at −30 °C.[56] Full conversion was obtained after ca. 15−20 min. A sample was withdrawn from the reaction mixture and analyzed by SEC and MALDI-TOF MS (see Figures S1 and S2 in the Supporting Information). The precursor polymers had molecular weights between 7000 and 9000 g·mol^{-1} and their MWDs were very narrow ($M_w/M_n = 1.04-1.05$). As we reported earlier, well-defined P*t*BA precursors could be obtained in a similar way,[57] and their molecular weights were between 4000 and 6000 g·mol^{-1} with narrow MWD, $M_w/M_n = 1.10-1.18$ (see Figures S3 and S4 in the Supporting Information). Polymerization of *t*BA occurred within 1 min at −78 °C. By using the absolute number-average molecular weights, M_n, measured by MALDI-TOF MS, high initiator efficiencies were calculated and are in the range between 0.8 and 1.0. The effective P*t*BMA-Li, and P*t*BA-Li chain end concentrations for the initiation of the second monomer can be calculated by taking the molecular weight given by MALDI-TOF (see Table S1 in the Supporting Information). The livingness of the *t*BMA polymerization was investigated by in-line FT-NIR spectroscopy coupled with SEC and MALDI-TOF mass spectrometry. The same treatment is not possible for the *t*BA polymerization because the half-lives are too short to allow for sample withdrawing during the course of the polymerization ($t_{1/2} \approx 10$ s).

As shown in Figure 5 for the polymerization of *t*BMA at −30 °C (run J), a linear first-order time-conversion plot is observed and the molecular weight determined by MALDI increases linearly with the conversion, X_p, while the polydispersity index, M_w/M_n, decreases with conversion. It indicates the livingness of the *t*BMA polymerization under these conditions. An apparent polymerization rate, $k_{app} = 4.9\cdot10^{-3}$ s^{-1}, and an absolute polymerization rate constant, $k_p = k_{app}/(f\cdot[I]_0) = 3.0$ L·mol^{-1}·s^{-1}, can be calculated. The latter compares well to the previously reported data by Kunkel et al., $k_p = 3.5$ L·mol^{-1}·s^{-1} for the polymerization of *t*BMA initiated by methyl α-lithioisobutyrate (MiBLi) in THF at −30 °C using a similar ratio $[\text{LiCl}]/(f\cdot[\text{MiBLi}]_0) = 16.6$.[58]

The initiation of DEAAm by various P*t*BA-Li macroinitiators was observed in THF at −78 °C, and P*t*BA-*b*-PDEAAm copolymers were obtained. Nevertheless, the method suffered from a low blocking efficiency ($f = 0.15-0.31$), as summarized in Table 2 (runs G, H, and I). We initially attributed this to the short livingness of P*t*BA-Li active chains after complete monomer conversion, leading to the deactivation of the active centers by backbiting termination before addition of the second monomer.[57] This can be easily observed in the SEC traces of the block copolymer at different DEAAm conversions, where a second peak attributed to the remaining precursor is present (Figure 6A). To circumvent this crucial problem, we decided to use P*t*BMA-Li as a macroinitiator, which is known to be more stable than P*t*BA-Li in THF at low temperature. *t*BMA was polymerized at −30 °C in order to achieve complete *t*BMA conversion in a reasonable time. Despite the fact that the polymerization of *t*BMA occurs in a living fashion in THF at −30 °C, and that DEAAm was consumed quantitatively, blocking efficiencies are in the range $0.40 \le f \le 0.70$ only. The SEC traces of the resulting crude copolymer are bimodal (Figure 7), corresponding to a considerable amount of P*t*BMA

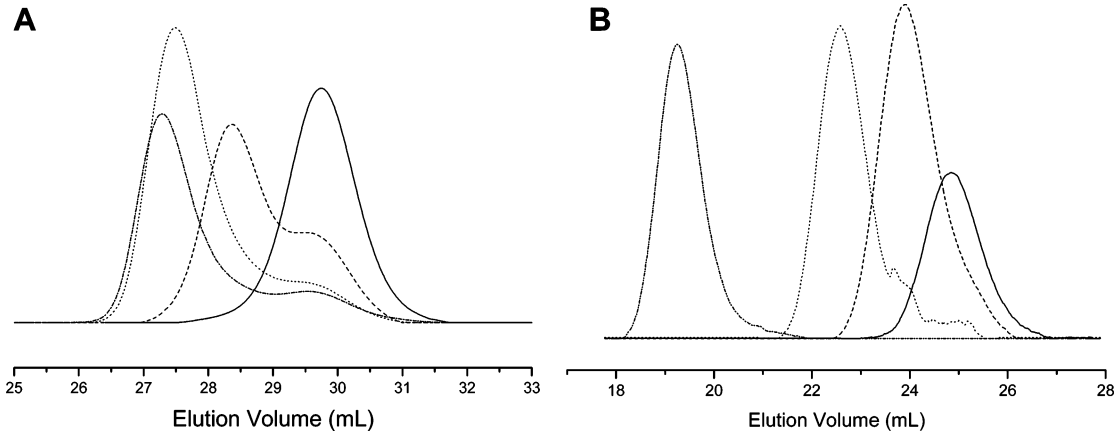

Figure 6. (A) SEC traces (normalized RI signal) of the P*t*BA precursor (—), and the crude P*t*BA-*b*-PDEAAm copolymers before purification at 0.34 (- - -), 0.84 (···), and 1.0 (-···-) of DEAAm conversion for run G. The SEC measurements were performed in THF +0.25 wt % tetrabutylammonium bromide (TBAB) at 23 °C.[57] (B) SEC traces of purified P*t*BMA-*block*-PDEAAm copolymers synthesized in THF at −78 °C using different initial DEAAm concentrations: $[DEAAm]_0 = 11.2$ (—, run J), 44.7 (- - -, run K), 89.9 (···, run L), 202.4 mmol·L^{-1} (-···-, run M). Experimental conditions: see Table 2.

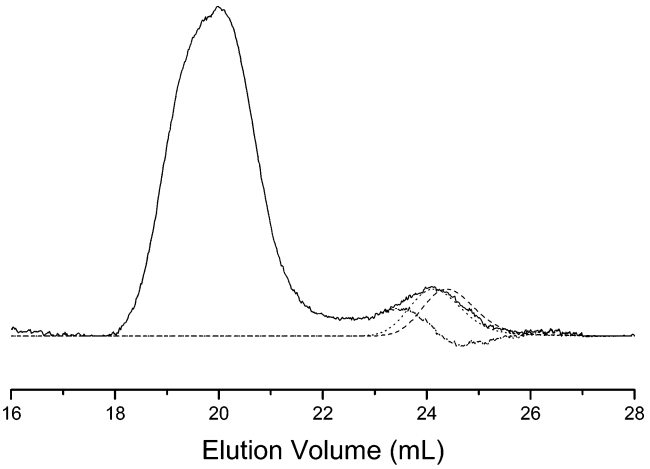

Figure 7. SEC (in THF, RI signal) traces of the P*t*BMA precursor (—) and the crude P*t*BMA-*b*-PDEAAm (- - -) for $X_p = 0.56$. A shift of the precursor peak by 0.30 mL (···) enables the subtraction from the block copolymer peak (-·-·-·), run M. Experimental conditions, see Table 2.

homopolymer. This might suggest that significant self-termination takes place before initiation of the polymerization by P*t*BMA-Li, as it was observed using P*t*BA precursors. However, P*t*BMA-Li chain ends were reported to be quite stable at $T \leq -30$ °C. For both P*t*BA-Li and P*t*BMA-Li macroinitiators, the lowest blocking efficiencies are observed with the highest ratios $r^* = [Et_3Al]_0/[P^*]_0$.

The SEC traces (RI detection) indicate a shift of the maximum attributed to the P*t*BMA precursor from $V_{max} = 24.4-24.1$ mL in the copolymer trace (Figure 7), i.e., subtraction of the precursor peak is only possible if the precursor is somewhat shifted toward higher molecular weights, indicating that it could have added one or two DEAAm units before terminating.

The UV traces at $\lambda = 270$ and 300 nm are shown in Figure 8. No signal at $\lambda = 300$ nm is observed for the P*t*BMA precursor, whereas a noisy signal of low intensity is observed in the crude block copolymer that we attribute to the backbiting product of amidoenolate chains, i.e., a cyclic, enolized β-ketoamide,[5] similar to the enolized cylic β-ketoester observed in the polymerization of *n*-butyl acrylate[59] and *t*BA,[60] having strong UV absorption at 260 nm. Similarly, the formation of cylic β-ketoesters was reported as a backbiting product for the polymerization of MMA with an absorption at 300 nm.[61] The low signal-to-noise ratio is due to the relatively low absorbance of this cyclic product. We speculate that backbiting may occur after incorporation of one or two DEAAm units in the chain, as shown in Scheme 4. Indeed, the molecular weight at peak maximum is shifted from 9200 to 10 600 using a PS calibration, at shown in Figure 7. As indicated in Scheme 4, the driving force for the termination process is probably due to the presence of the acidic α-proton ($pK_a = 12-14$)[62] in the newly formed cyclic β-ketoamide, which induces the termination of a second PDEAAm-Li growing chain, the resulting anion of the cyclic β-ketoamide being not nucleophilic enough to initiate the polymerization. The residual active chain end concentration is assumed to remain stable during the polymerization of DEAAm, allowing living polymerization as discussed below. Nevertheless, by precipitation of the reaction mixture in *n*-hexane after quenching, it is possible to eliminate the remaining precursor and the copolymer chains containing a few units of DEAAm to yield pure diblock copolymers, as shown in Figure 6B.

2. Polymerization Kinetics. The course of the polymerization was followed by in situ FT-NIR spectroscopy, and samples were taken at various monomer conversions for the experiments with $t_{1/2} > 1$ min. The decrease of the intensity of the bands with time was followed. Specific monomer absorptions for DEAAm were detected at ca. 6156, 6071, 6001, 4748, 4713, 4686, 4621, and 4574 cm^{-1} (Figure 9). In contrast to the RAFT polymerization of NIPAAm in dioxane, no absorption attributed to the polymer at ca. 6700 cm^{-1} was found.[35] The strongest vibration located at ca. 6156 cm^{-1} was attributed to the first overtone of C−H vinylic stretching of DEAAm. Furthermore, this specific vibration is well separated from other vibrations or solvent cutoff, and therefore, its peak height was chosen for conversion determination. Peak heights are generally used instead of peak areas for evaluation because they usually give less noise. The monomer conversions, X_p, were calculated using eq 2:

$$X_p = \frac{A_0 - A_t}{A_0 - A_\infty} \tag{2}$$

where A_t is the absorbance at time t, A_0 is the initial absorbance, and A_∞ is the absorbance at full conversion.

(i) Effect of Monomer Concentration. Four different kinetic runs were carried out using P*t*BMA-Li living chains as a macroinitiator for the anionic polymerization of DEAAm in the presence of Et_3Al. The effect of the initial monomer concentra-

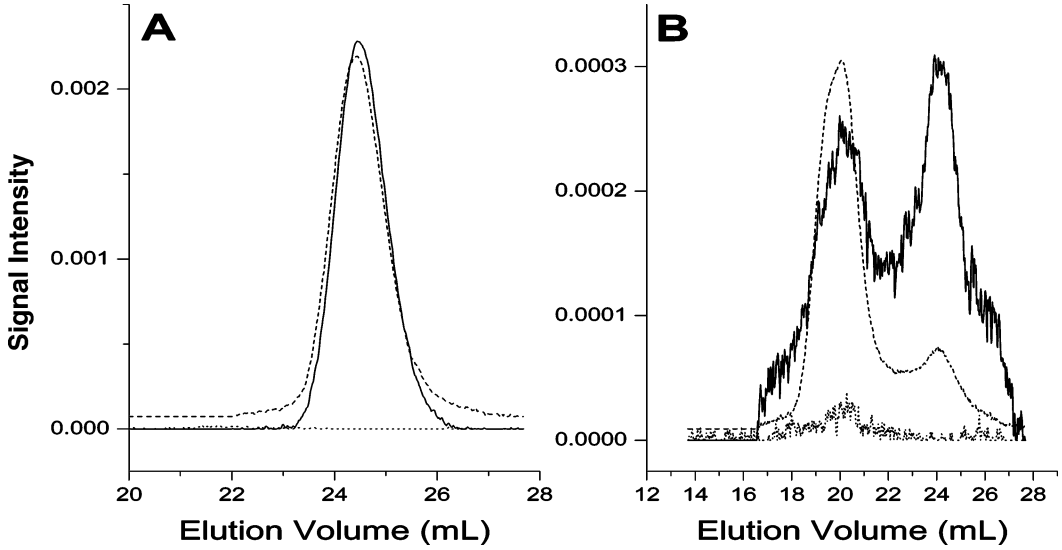

Figure 8. SEC traces of the P*t*BMA precursor (A) and the crude P*t*BMA-*b*-PDEAAm for $X_{p,DEAAm} = 0.56$ (B) in NMP + LiBr at 70 °C. RI detection (- - -), UV detection at $\lambda = 270$ (—) and 300 nm (···). Run M, experimental conditions: see Table 2.

Scheme 4. Aggregation of the Amidoenolate Chain Ends in the Absence of Et_3Al

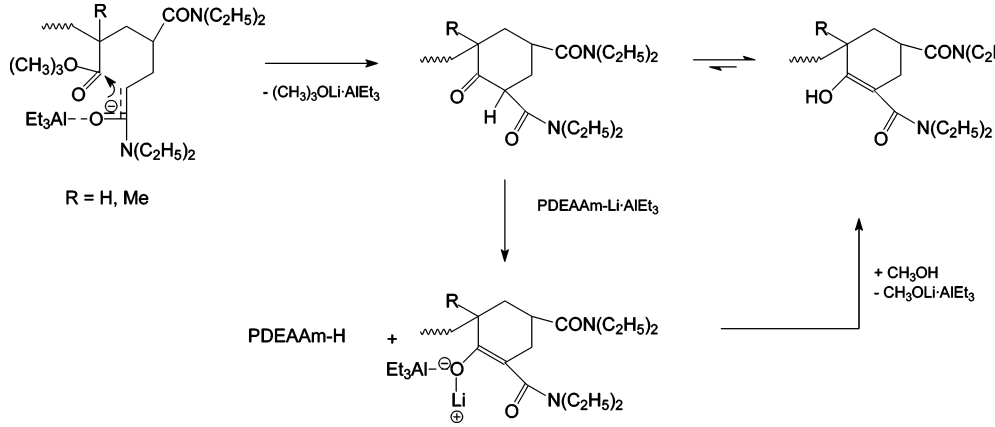

tion on the polymerization kinetics was examined, keeping the other concentrations ([P*t*BMA-Li]$_0$, [Et_3Al]$_0$) constant. These series of experiments were carried out in the presence of LiCl, the effect of which is a priori considered as negligible in contrast to the strong effect of aluminum alkyl. This assumption is confirmed below. Table 3 summarizes the experimental conditions and the kinetic data obtained for the four different experiments. The plots of monomer conversion vs time show a high linearity up to high conversion $X_p \leq 0.9$ (Figure 10). At first glance, this suggests an internal zeroth order with respect to [DEAAm]$_0$. Moreover, the slopes in this plot decrease with increasing initial monomer concentration, which can be regarded as a negative reaction order with respect to monomer.

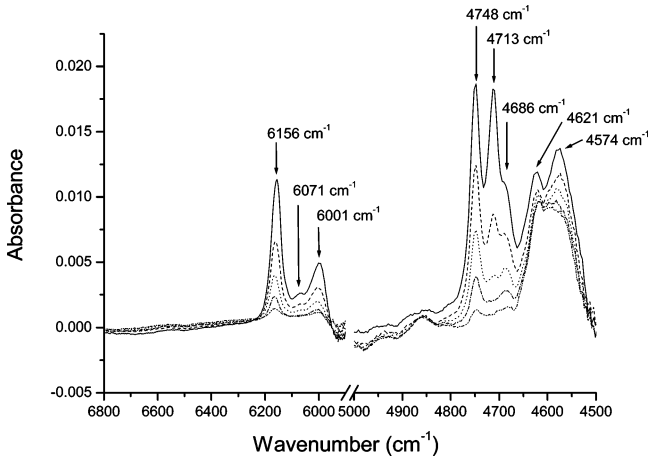

Figure 9. Evolution of various NIR vibration overtone bands obtained after solvent subtraction at $t = 0$, 7.4 (- - -), 14.8 (···), 22.3 (-·-), and 33.3 s (-··-) for the polymerization of DEAAm initiated by EiBLi/Et_3-Al in THF at $T = -78$ °C (run E). Experimental conditions: [DEAAm]$_0$ = 45.4 mmol·L^{-1}, [EiBLi]$_0$ = 1.14 mmol·L^{-1}, [Et_3Al]$_0$ = 19.0 mmol·L^{-1}.

The first-order time-conversion plots show an upward curvature for all runs except for the lowest [DEAAm]$_0$, where [Et_3Al]$_0 \approx$ [DEAAm]$_0$ (Figure 10B). The same feature was observed using a P*t*BA-Li macroinitiator (see Figure S7 in the Supporting Information). The number-average molecular weights increase linearly with monomer conversion (Figure 11), and the final block copolymers after purification have narrow MWDs. This excludes the hypothesis of a slow initiation, which also would result in a sigmoidal shape of the linear plot of conversion vs time that is not observed.

The observed polymerization rate constants in the final state, $k_{p,exp} = k_{app}^{(2)}/[P^*]_0$, only show a slight decrease when [DEAAm]$_0$ increases, but this is only due to the effective active chain end concentration, $[P^*]_0 = f \cdot [I]_0$, which varies for each run. Figure 12 shows that the rates, when normalized to the effective chain end concentration, $[P^*]_0 = f \cdot [I]_0$, are constant within the limits of experimental error. Thus, only the *initial* rates (at higher monomer concentrations) depend on [DEAAm]$_0$.

Table 3. Experimental Conditions and Kinetic Results of DEAAm Polymerization Using Various Initial Monomer Concentrations in THF at −78 °C[a]

run	$[I]_0$[b] mmol·L^{-1}	$[M]_0$ mmol·L^{-1}	r $= [Et_3Al]_0/[I]_0$	$[M]_0/[Et_3Al]_0$	f[c]	$[P^*]_0$[d] mmol·L^{-1}	$10^2 \cdot k_{app}^{(1)}$[e] s^{-1}	$10^2 \cdot k_{app}^{(2)}$[e] s^{-1}	$k_{p,exp}$[f] L·(mol·s)$^{-1}$
J	1.62	11.2	7.72	0.89	0.70	1.13	11.2	11.2	99.4
K	1.71	44.7	7.31	3.54	0.40	0.68	4.60	7.82	115
L	1.51	89.9	8.34	7.19	0.53	0.80	3.13	7.67	95.9
M	1.38	202	9.13	16.2	0.42	0.58	0.73	5.18	89.3

[a] $[Al] = [Et_3Al]_0 = 12.6$ mmol·L. [b] $[I]_0 = [PtBMA\text{-}Li]_0$, see Table 2. [c] Blocking efficiency, see Table 2, $f = (M_{n,theo} - M_{n,MALDI,prec})/(M_{n,MALDI} - M_{n,MALDI,prec})$. [d] Effective chain end concentration, $[P^*]_0 = f \cdot [I]_0$. [e] Initial and final slopes of the first-order plots. [f] Observed rate constant at high conversion, $k_{p,exp} = k_{app}^{(2)}/[P^*]_0$.

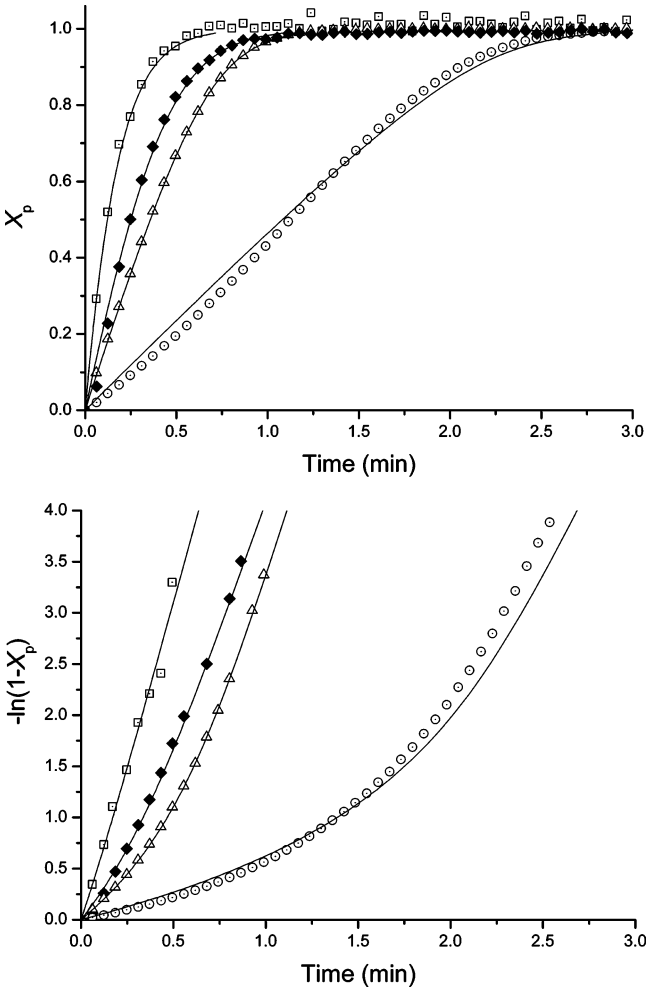

Figure 10. Linear (top) and first-order (bottom) time-conversion plots for the anionic polymerization of DEAAm at −78 °C with P*t*BMA-Li/Et_3Al in THF using different initial monomer concentrations: $[DEAAm]_0 = 11.2$ (□), 44.7 (■), 89.9 (△), 202.4 (○) mmol·L^{-1} (runs J, K, L, and M). For reaction conditions, see Table 3. The lines are fits according to Scheme 1a,b and the kinetic model outlined below (Scheme 6) with $K_M = 10^3$ and $K_{CE} = 10^2$, $k'_{\pm} = 220$ L·mol^{-1}s^{-1}.

The observation that an internal zeroth order with respect to the actual monomer concentration $[DEAAm]_t$ might be explained by the activation of DEAAm by Et_3Al, i.e., mainly activated monomer contributing to propagation and the concentration of *activated* monomer being constant up to high conversion, if Et_3Al is liberated after monomer addition to activate another monomer molecule. The ^{13}C NMR spectra of the carbonyl region of DEAAm are shown in Figure 13. In the absence of Et_3Al, the chemical shift of the peak attributed to the DEAAm carbonyl carbon is 164.82 ppm. In THF-d_8, the Et_3Al/DEAAm solution is slightly turbid ($[Et_3Al]_0/[DEAAm]_0 = 1$), and the peak attributed to the carbonyl group is shifted downfield ($\delta = 174.05$ ppm), indicating that the electron density of the carbonyl carbon is lowered due to the coordination to Et_3Al. A similar effect was observed by Aida et al. and by Schlaad et al. for methyl methacrylate (MMA) complexed by bis[triisobutyl(phenoxy)] methylaluminum in dichloromethane[63] or trimethyl- and triisobutylaluminum in toluene,[64] respectively. The slight turbidity as well as the relatively broad shape of the peak may be attributed to the possible initiation of DEAAm by Et_3Al in the absence of an initiator. Indeed, precipitation of polymer was observed at the end of the measurement. Similarly, the slow polymerization of DEAAm in the presence of Et_3B in THF at 25 °C was reported by Kobayashi et al.[11] The relatively high concentration used for ^{13}C NMR measurement ($c = 100$ g·L^{-1}) may explain the occurrence of this phenomenon.

However, the assumption that mainly activated monomer is polymerized neither explains the increase of polymerization rates with the conversion nor the apparent negative reaction order of the initial reaction rates with respect to $[DEAAm]_0$. The experimental results indicate that the apparent rate constants increase constantly during the polymerization, i.e., with decreasing *actual* monomer concentration, $[DEAAm]_t$. This is shown in Figure 14, where the slopes of the first-order time-conversion plots, i.e., that *instantaneous* observed rate constants, $k_{app}(t)$, normalized to the same chain end concentration, $[P^*]_0$, are plotted versus the *instantaneous* monomer conversion $[DEAAm]_t$ at that time (this implies that polymerization kinetics is first-order with respect to the effective concentration of active centers, $[P^*]_0$, which is shown further below). Identical instantaneous rate constants are observed for $[DEAAm]_t < [Et_3Al]_0$, whereas they decrease at higher concentrations. This observation can be explained by taking into account that the equilibrium between free and activated monomer (Scheme 1c) has a DFT-calculated energy gain of ca. 7 kJ·moL^{-1}, indicating that the equilibrium is not completely shifted to the right-hand side, but depends on the ratio of monomer to Et_3Al, as shown in Scheme 5.

Because [THF] = const, we introduce the equilibrium constant $K = K_M/[THF] = K_M/12.5$ M. Then we can set up the mass action law,

$$K = \frac{[M]_{act}}{[M]_{free} \cdot [Et_3Al \cdot THF]} \tag{3}$$

and define the fraction of activated monomer, $\alpha_M = [M]_{act}/[M]_t$. The solution of the corresponding quadratic equation (for a more detailed discussion, see Supporting Information) renders

$$\alpha_M = \frac{1}{2} \cdot \left(1 + \frac{[Et_3Al]_0 + K^{-1}}{[M]_t}\right) - \sqrt{\left[\frac{1}{4} \cdot \left(\frac{[Et_3Al]_0 + K^{-1}}{[M]_t}\right)^2 - \frac{[Et_3Al]_0}{[M]_t}\right]} \tag{4}$$

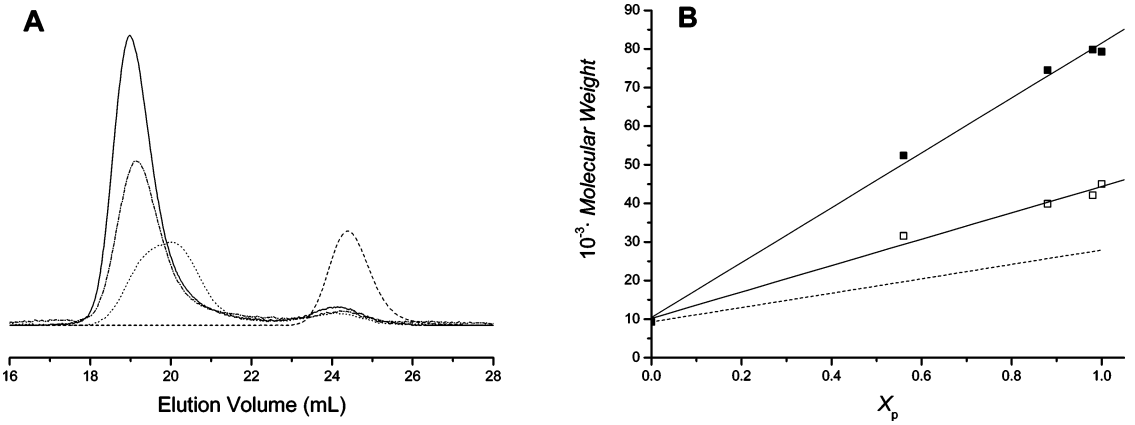

Figure 11. (A) SEC traces of the P*t*BMA precursor (- - -), and of the crude P*t*BMA-*b*-PDEAAm at $X_p = 0.56$ (···), 0.88 (-·-), 1.0 (—) (run M) in NMP + LiBr at 70 °C. The RI signals are normalized according to the weight of incorporated DEAAm. (B) Dependence of M_n (□) and M_{peak} (■) (SEC) on DEAAm conversion for run M using P*t*BMA-Li as macroinitiator in the presence of Et_3Al and LiCl in THF at −78 °C. For experimental conditions, see Table 3. The absolute molecular weights are corrected from the molecular weights obtained with a PS calibration in NMP + LiBr, using eq 1. The theoretical evolution of the molecular weights is shown as a dotted line.

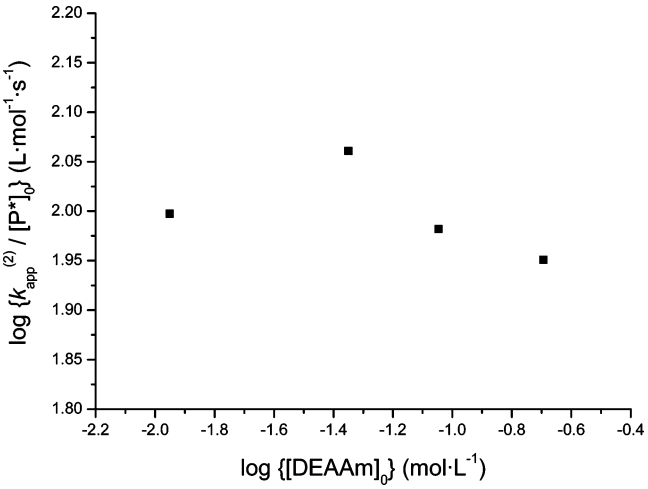

Figure 12. Determination of the external reaction order with respect to the initial monomer concentration, $[DEAAm]_0$, for the anionic polymerization of DEAAm with P*t*BMA-Li/Et_3Al in THF at −78 °C. The apparent rate constants, $k_{app}^{(2)}$, were determined at high conversion. Slope = $-0.04 \pm 0.05 \approx 0$. Experimental conditions: $[DEAAm]_0$ = 11.2−202 mmol·L^{-1}, $[P$*t*BMA-Li$]_0$ = 1.38−1.71 mmol·L^{-1}, $[Et_3Al]_0$ = 12.6 mmol·L^{-1}.

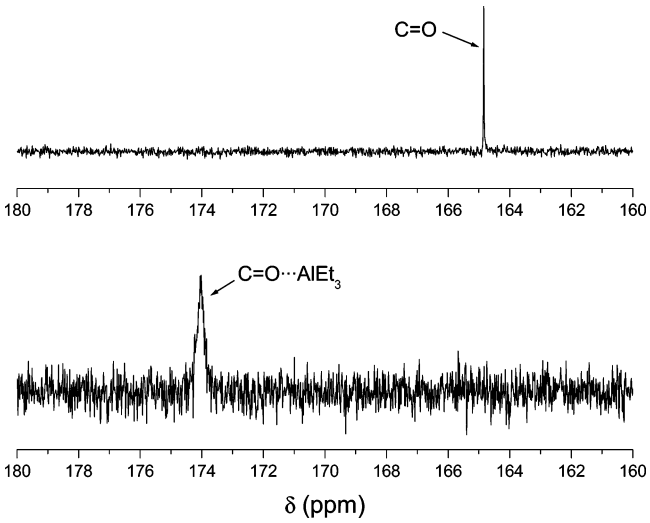

Figure 13. ^{13}C NMR spectra of the carbonyl region of DEAAm in the absence (top) and presence of Et_3Al (bottom) in THF-d_8, $[Et_3Al]_0/[DEAAm]_0 \approx 1$.

The limiting relationships are

$$[M]_t \gg [Et_3Al]_0 \Rightarrow \alpha \sim [M]_t^{-1}$$

$$[M]_t \ll [Et_3Al]_0 \Rightarrow \alpha \sim K\cdot[Et_3Al]_0/(1 + K\cdot[Et_3Al]_0) \approx K\cdot[Et_3Al]_0 \quad (5)$$

The observed instantaneous rate constant, $k_{p,exp} = k_{app}/[P^*]_0$, can than be seen as composed of those of the activated and the free monomer, k_p' and k_p, respectively:

$$k_{p,exp} = \alpha_M\cdot k_p' + (1 - \alpha_M)\cdot k_p \quad (6)$$

For $k_p' \gg k_p$ and not too small α_M, this leads to $k_{p,exp} \cong \alpha_M\cdot k_p'$, i.e., the observed rate constant, should be directly proportional to α_M.

The dependence of the fraction of activated monomer, α_M, is plotted in Figure 15 for various values of K. It is seen that α_M increases with decreasing monomer concentration and levels off when the monomer concentration reaches the level of $[Et_3Al]_0$. A reasonable fit of the data in Figure 14 is obtained for $K_M \cong 10^3$, where both the k_{app} and α_M values at the highest and lowest monomer concentration span 1 order of magnitude. Moreover, a very good fit of the time conversion plots (Figure 10) is observed with this value of equilibrium constant (as will

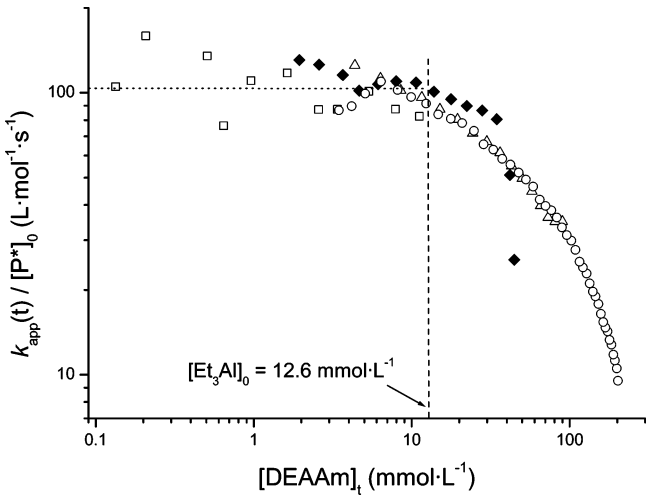

Figure 14. Dependence of the instantaneous observed rate constant, $k_{p,exp} = k_{app}(t)/[P^*]_0$, on the actual monomer concentration $[DEAAm]_t$. Symbols, see Figure 10. Experimental conditions: see Table 3.

Table 4. Experimental Conditions and Kinetic Results of DEAAm Polymerization Using Various Initial Initiator Concentrations, $[EiBLi]_0$, in THF at − 78 °C[a]

run	$[I]_0$[b] mmol·L^{-1}	$r = [Et_3Al]_0/[I]_0$	$r^* = [Et_3Al]_0/[P^*]_0$	f[c]	$[P^*]_0$[d] mmol·L^{-1}	$t_{1/2}$ s	$10^2 \cdot k_{app}$[e] s^{-1}	$k_{p,exp}$[f] L·(mol·s)$^{-1}$
C	0.63	29.8	134	0.23	0.14	21.6	3.63	259
E	1.14	16.7	73.1	0.23	0.26	6.6	9.50	365
F	1.69	11.1	22.7	0.49	0.83	3.0	31.6	381

[a] Initial monomer concentration, $[DEAAm]_0 = 44.8-45.4$ mmol·L^{-1}, $[Et_3Al]_0 = 18.8-19.0$ mmol·L^{-1}, $[DEAAm]_0/[Et_3Al]_0 = 2.4$. [b] Initial initiator concentration, $[I]_0 = [EiBLi]_0$. [c] Initiator efficiency. [d] Effective chain end concentration, $[P^*]_0 = f \cdot [I]_0$. [e] Slope of the first-order plot. [f] Observed rate constant, $k_{p,exp} = k_{app}/[P^*]_0$.

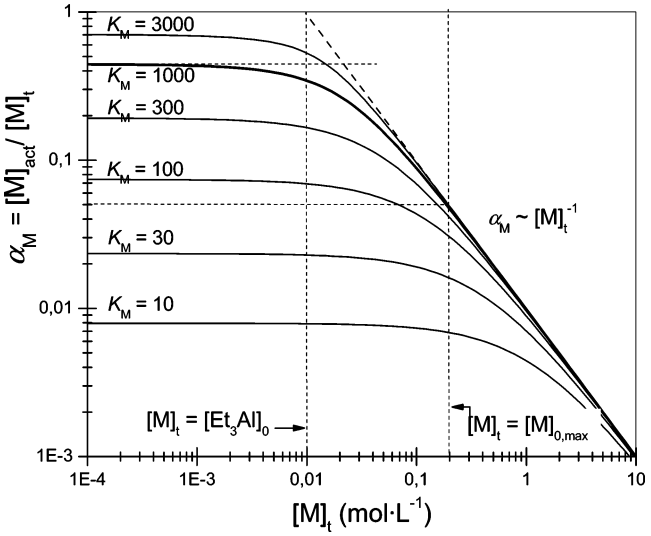

Figure 15. Dependence of the fraction of activated monomer on the instantaneous monomer concentration, calculated according to eq 4 for $[Et_3Al]_0 = 10$ mM. The dotted vertical lines indicate the maximum monomer concentration used in our experiments and the point, where the monomer concentration is equal to $[Et_3Al]_0$, the horizontal dotted lines show that α_M drops from 0.45 to 0.05 for $K_M = 1000$ for the highest initial monomer concentration investigated.

be seen in Part iii, the shape of the time-conversion plot also depends on the equilibrium constant related to the complexation of the chain end, K_{CE}). The observation that a linear first-order time-conversion plot is observed for the lowest-initial-monomer concentration (run J, $[DEAAm]_0 = 11$ mM $\cong [Et_3Al]_0$) can easily be explained by the fact that, below that, α_M does not change very much any more. For the estimated equilibrium constant, $K_M \cong 10^3$, we can calculate the free energy difference as $\Delta G \cong -11$ kJ·moL^{-1}. Assuming that there is no large entropy change (same number of reagents in educts and products), this coincides quite well with the value of $\Delta E = -7$ kJ·moL^{-1} calculated by DFT for the reaction of DMAAm with Et_3Al·THF (Scheme 1c).

Up to now, our experimental observations are in agreement with a combination of Schemes 5 and 6, the latter scheme illustrating the various equilibria the chain end is involved in. In the absence of a Lewis base, we have a coexistence of associated and free ion pairs, which are believed to be in a slow equilibrium, similar to the case of acrylates and methacrylates in THF;[65,66] however, according to the DFT calculations, the equilibrium is quite shifted toward the free ion pairs. Thus, the main contribution to propagation is related to the rate constant

Scheme 5. Equilibrium between Free and Activated Monomer

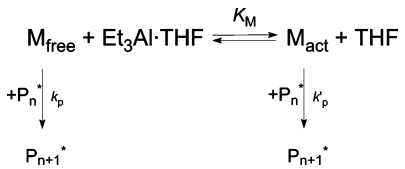

Scheme 6. Postulated Mechanism of DEAAm Polymerization in THF with $k_{\pm} \gg k_c \gg k_{ass}$, $k'_{\pm} \gg k_{\pm}$, and $k'_c \gg k_c$

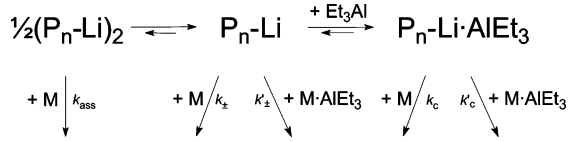

of noncomplexed ion pairs, $k_{\pm}$. In the presence of the Lewis base, this equilibrium will shift to the right-hand side, and aggregates disappear completely. How much the equilibrium of complexation with Et_3Al is shifted to the right-hand side depends on the related equilibrium constant, K_{CE}, and will be discussed further below (Part iii). Because the complexed chain end is much less reactive than the free one, the main contribution will be related to the rate constant of addition of activated monomer to noncomplexed ion pairs, $k'_{\pm}$.

(ii) Effect of Initiator Concentration. The initial concentrations of Et_3Al, and DEAAm were maintained constant while varying the initial concentration of EiBLi in THF at −78 °C. These series of experiments were carried out in the absence of LiCl. The results are collected in Table 4. Linear first-order time-conversion plots are observed in all the cases (Figure 16). Here, the ratio, $[DEAAm]_0/[Et_3Al]_0 = 2.4$, is constant, i.e., the initial monomer concentration is not much higher than $[Et_3Al]_0$ and strong deviations from linearity are not expected. Because of the very fast polymerizations obtained using EiBLi as an initiator ($t_{1/2} < 22$ s), withdrawing samples was impossible. Using P*t*BMA-Li or P*t*BA-Li as a macroinitiator, the observed polymerization rate constant, $k_{p,exp} = k_{app}/[P^*]_0$ is lower than that observed with EiBLi as an initiator. This is attributed to the presence of LiCl in the solution for the polymerization of

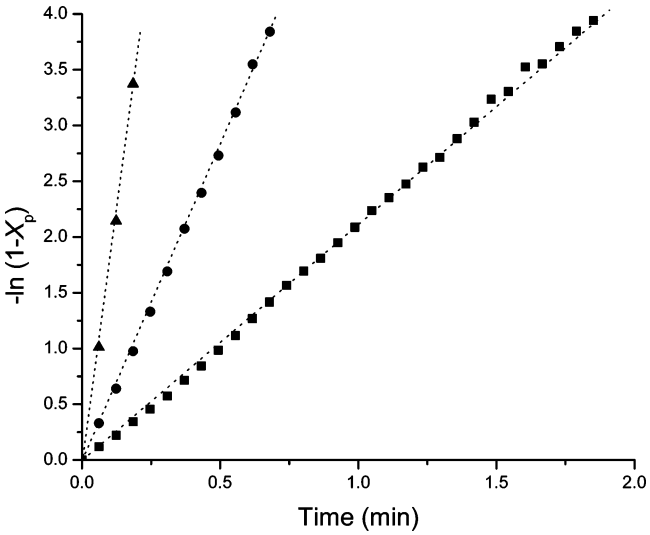

Figure 16. First-order time-conversion plots for the anionic polymerization of DEAAm initiated by EiBLi/Et_3Al in THF at −78 °C using various initial initiator concentrations: (▲) 1.69, (●) 1.14, and (■) 0.63 mmol·L^{-1}. Reaction conditions, see Table 4.

Table 5. Experimental and Kinetic Data of DEAAm Polymerization Using Different Et_3Al Concentration in THF at −78 °C[a]

run	$[I]_0$[b] mmol·L^{-1}	$[Et_3Al]_0$ mmol·L^{-1}	$r = [Et_3Al]_0/[I]_0$	$r^* = [Et_3Al]_0/[P^*]_0$	$[M]_0/[Et_3Al]_0$	f[c]	$[P^*]_0$[d] mmol·L^{-1}	$t_{1/2}$ s	$10^2 \cdot k_{app}$[e] s^{-1}	$k_{p,exp}$[f] L·(mol·s)$^{-1}$
A	0.87	0	0	0	-	0.41	0.36	1.20	24.6	680
B	0.65	4.7	7.23	21.3	9.51	0.34	0.22	18.6	14.7[g] (3.28)[h]	670 (150)[i]
C	0.63	18.8	29.8	130	2.37	0.23	0.14	21.6	3.63	260
D	0.74	30.8	41.6	160	1.45	0.20	0.15	21.6	2.95	200

[a] Initial monomer concentration, $[DEAAm]_0 = [M]_0 = 44.1-45.3$ mmol·L. [b] Initial initiator concentration, $[EiBLi]_0 = [I]_0$. [c] Initiator efficiency, $f = M_{n,theo}/M_{n,MALDI}$, see Table 1. [d] Effective chain end concentration, $[P^*]_0 = f \cdot [I]_0$. [e] Slope of the first-order plot. [f] Observed rate constant at high conversion, $k_{p,exp} = k_{app}/[P^*]_0$. [g] At high conversion. [h] At low conversion. [i] Calculated with the slope at low conversion.

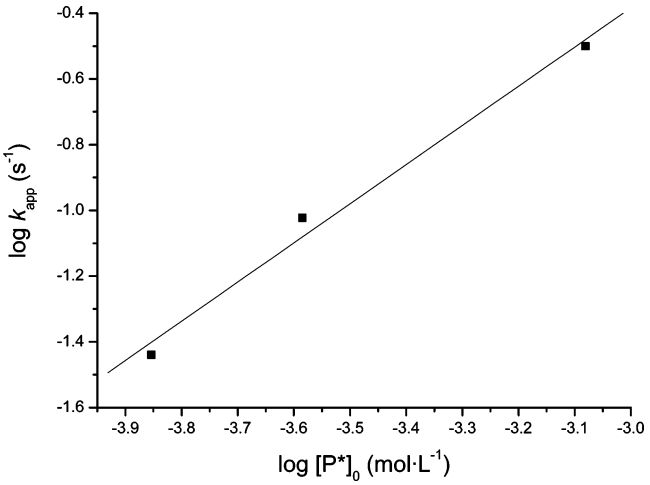

Figure 17. Determination of the external reaction order with respect to the effective concentration of active centers, $[P^*]_0$, for the anionic polymerization of DEAAm with EiBLi/Et_3Al in THF at −78 °C. Slope = 1.19 ± 0.13.

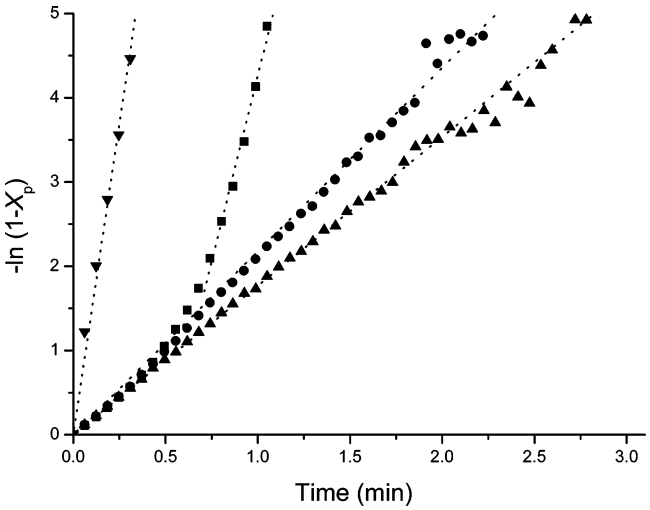

Figure 18. First-order time-conversion plots for the anionic polymerization of DEAAm initiated by EiBLi in THF at −78 °C using various Et_3Al concentrations, $[Et_3Al]_0$: (▼) 0, (■) 4.7, (●) 18.8, and (▲) 30.8 mmol·L^{-1}. Reaction conditions: $[DEAAm]_0 = 44.1-45.3$ mmol·L^{-1}, $[I]_0 = 0.65-0.87$ mmol·L^{-1} (runs A, B, C, and D).

DEAAm initiated by P*t*B(M)A-Li macroinitiator. Even if LiCl tends to dissociate the aggregates in the polymerization of alkyl methacrylate monomers in THF,[65] this effect was not observed for DEAAm and DMAAm, where broad MWDs were found even in the absence of Lewis acid.[6]

The bilogarithmic plot in Figure 17 indicates that the reaction is first-order with respect to the effective concentration of active centers, $[P^*]_0 = f \cdot [I]_0$. This is expected because the initiator concentration does not enter into the equation for α_M.

(iii) Effect of Et_3Al Concentration. In a third series of experiments, the initial concentration of Et_3Al was varied, keeping the other concentrations constant. EiBLi was used as an initiator in THF at −78 °C in the absence of LiCl. The results are given in Table 5. The first-order time-conversion plots are always linear in the absence or in the presence of Et_3Al except for run B ($[Et_3Al]_0 = 4.7$ mmol·L^{-1}), where $[DEAAm]_0/[Et_3Al]_0 = 9.5$ (Figure 18). At this ratio, a similar behavior as in Part i is expected, whereas, in the other two cases, the ratio $[DEAAm]_0/[Et_3Al]_0 < 2.4$, similar to the case in Part (ii). In the absence of Et_3Al, a very fast reaction occurs and a broad MWD is observed (Table 1, run A). Because association should not be very pronounced, the broad MWD might be explained by the poor solubility of the polymers in THF, leading to a heterogeneous reaction.

Upon addition of Et_3Al, narrow MWDs are observed (Figure 1), and the polymerization rates decrease, which is in accordance with previous work on aluminum−esterenolate complexes in toluene that are known to polymerize more slowly than noncoordinated esterenolate.[28] The dependence of the polymerization rate constant on $[Et_3Al]_0$ was examined. For $[Et_3Al]_0/[P^*]_0 > 5$, the observed rate constants (calculated at high monomer conversion), $k_{p,exp}$, gradually decrease to ca. 30% of the initial value without Et_3Al with an external order of −0.7 (Figure 19).

However, this observation is in contradiction to the calculations on the fraction of activated monomer (eqs 4−6). Equation 5 predicts that the concentration of activated monomer increases with increasing $[Et_3Al]_0$, and consequently, the rate should increase, too. Thus, we must now examine how the concentration of complexed (less active) chain ends depends on $[Et_3Al]_0$. On the basis of Scheme 1b (see also the right part of Scheme 6), we can calculate the fraction of complexed chain-ends, α', in a similar way as for the fraction of activated monomer (see Supporting Information, eq S8). Unfortunately, the equation is more complex and depends on both equilibrium constants for the activation of monomer, K_M (Scheme 5), and deactivation of chain ends, K_{CE} (Scheme 6). The fraction of active, noncomplexed species, $1-\alpha'$, is given in Figure 20. We see that the dependence is similar to the observation in Figure 19, with a slope of −1 in the bilogarithmic plot. Thus, we must conclude that the kinetics of this system is governed by a complex interplay between the activation of the monomer and the deactivation of chain ends. At low ratios $r = [Et_3Al]_0/[I]_0$, the effects of monomer activation seem to approximately cancel, whereas at higher r values, the fraction of activated monomer is close to unity and the effect of chain end deactivation prevails.

Thus, at a given set of initial concentrations of monomer, initiator, and Et_3Al, the observed rate constant depends on six parameters (see Scheme 6), α_M, α', $k_\pm$, $k'_\pm$, k_c and k'_c:

$$k_{p,exp} = [\alpha_M \cdot k'_\pm + (1 - \alpha_M) \cdot k_\pm] \cdot (1 - \alpha') + [\alpha_M \cdot k'_c + (1 - \alpha_M) \cdot k_c] \cdot \alpha' \quad (7a)$$

where both α_M and α', (and consequently $k_{p,exp}$) depend on monomer conversion. Even if we neglect the contribution of

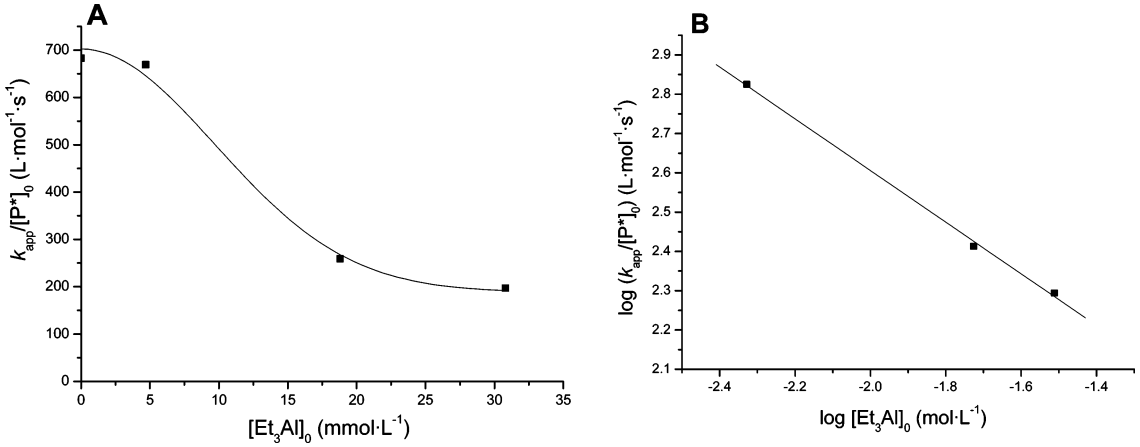

Figure 19. (A) Dependence of the observed rate constant (at high conversion), $k_{p,exp} = k_{app}/[P^*]_0$, on $[Et_3Al]_0$. (B) Determination of the external reaction order with respect to the concentration of Et_3Al for the anionic polymerization of DEAAm with EiBLi in THF at −78 °C. Slope = −0.66 ± 0.03.

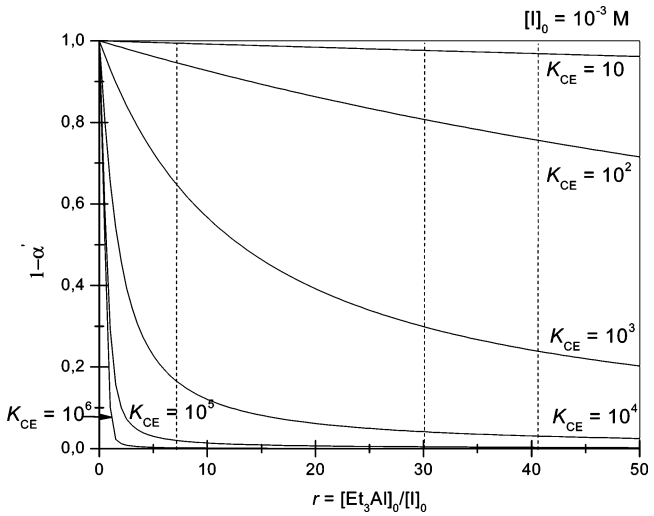

Figure 20. Calculated fraction of active (noncomplexed) chain ends, 1-α′, as a function of the ratio $[Et_3Al]_0/[I]_0$ at high monomer conversion ($[M] \ll [Et_3Al]_0$). The dotted lines correspond to the experimental ratios.

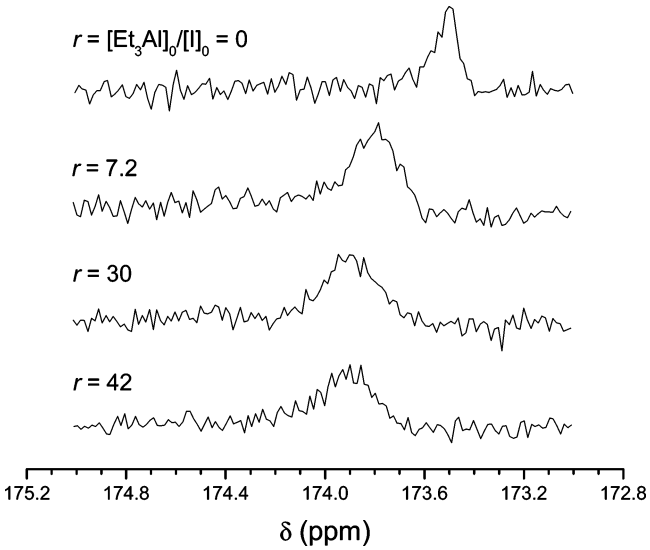

Figure 21. ^{13}C NMR spectra of the carbonyl region of the PDEAAms obtained with EiBLi/Et_3Al using various concentrations of Et_3Al. Reaction conditions: $[EiBLi]_0 = 0.65-0.87$ mmol·L^{-1}, $[DEAAm]_0 = 44.1-45.3$ mmol·L^{-1} (runs A, B, C, and D).

the deactivated chain ends to propagation (i.e., k_c and $k'_c = 0$), we end up with the four-parameter equation,

$$k_{p,exp} = [\alpha_M \cdot k'_{\pm} + (1 - \alpha_M) \cdot k_{\pm}] \cdot (1 - \alpha') \qquad (7b)$$

We tried to fit the various constants to the data in Figure 19. However, the number of data points and their accuracy is not high enough to allow for a reasonable fit. More measurements are necessary and will be performed in the future. In addition, even more can be learned from the temperature dependence of the various parameters.

The DFT-calculated energies of complexation range from −9 to −24 kJ·moL^{-1}, depending on the tacticity of the chain end (the implications for tacticity are discussed in a separate publication).[44] Again, neglecting entropy contributions, this translates into the equilibrium constant, K_{CE}, being in the range from 10^2 to 10^6. As is seen from Figure 20, K_{CE} values are in the range from 10^2 to 10^4, leading to a significant decrease of the concentration of noncomplexed chain ends in the range of Et_3Al concentrations investigated. It must be noted that the calculations in Figure 20 are simplified in neglecting the effect of monomer complexation (in fact, the fraction of active chain ends decreases with conversion, see Figure S9, Supporting Information) but they may serve for a semiquantitative estimation. The time-conversion plots in Figure 10 could, however, be fitted using $K_M = 10^3$ and $K_{CE} = 10^2$, but it should be noted that other sets of equilibrium constants also give a satisfactory fit.

3. Tacticity of PDEAAm. Previous studies indicated that the stereostructure of PDMAAm cannot be characterized by the *N*-methyl proton resonance, which shows complex patterns due to the combination of both the tacticity effect and the partially hindered rotation around the amide bond.[67] ^{13}C NMR spectroscopy of the carbonyl carbon gave better results for the assignment of configurations.[68] This methodology has been used in an efficient way to investigate the stereostructure of poly(*N,N*-dialkylacrylamide)s.[5,11] It is possible to assign the resonances of isotactic (*mm*, 173.3−173.6 ppm), heterotactic (*mr* + *rm*, 173.6−174.1 ppm), and syndiotactic triads (*rr*, 174.1−174.5 ppm) of PDEAAm carbonyl carbon signals.[6] In the absence of an additive, it was reported by Hogen-Esch that the isotactic triad fraction of PDMAAm decreased by decreasing the counterion size from cesium to lithium.[5] According to McGrath's, Hogen-Esch's, and Kobayashi's results,[4,6] PDEAAm produced with lithiated initiator in the presence or in the absence of LiCl is rich in isotactic configurations.

Figure 19 shows the ^{13}C NMR spectra of PDEAAm's produced with EiBLi in the absence and presence of various

amount of Et_3Al. The polymers produced with EiBLi in the absence of Et_3Al (run A) exhibit well-resolved carbonyl carbon signals in the region of 173.4−173.6 ppm, which are attributed to isotactic triads. Upon addition of Et_3Al ($r = 7.2$), a broad peak from 173.6 to 174.3 ppm emerges, which is attributed to heterotactic triads. This clearly indicates the influence of the additive on the monomer addition and the formation of the coordinated amidoenolate species. Similarly, Nakhmanovich et al. and Martinez-Castro et al. reported the highly heterotactic content of PDEAAm produced with DPHLi/Et_3Al[69] and PDMAAm produced with thienyllithium/Et_3Al, respectively.[70] An increase of r to 42 results in a slight shift toward the syndiotactic region (Figure 21). No change in the tacticity is observed for further addition of Et_3Al. These results are discussed in the light of DFT calculations in a separate publication.[44]

Conclusions

We have demonstrated that DEAAm could be successfully initiated by monomeric or polymeric lithium esterenolates in the presence of Et_3Al in THF at low temperature. For the synthesis of block copolymers, a poly(*tert* butyl acrylate)-Li or poly(*tert*-butyl methacrylate)-Li can be used as macroinitiator. The blocking efficiencies are rather low and attributed to a self-termination reaction occurring after incorporation of one or two DEAAm units. Kinetic studies, supported by quantum-chemical calculations, indicate a complicated mechanism involving equilibria between uncoordinated and Al-coordinated chain ends as well as between free and Et_3Al-activated monomer. The observed kinetics of this system is governed by a complex interplay between the activation of monomer (dependent on monomer and Et_3Al concentrations) and the deactivation of chain ends by complexation with Et_3Al (dependent on the ratio of concentrations of Et_3Al to initiator). Well-defined polymers rich in heterotactic ($mr + rm$) triads were synthesized, and they exhibit a cloud point in water at ca. 31 °C. Consequently, the poly[(meth)acrylic acid]-*block*-PDEAAm copolymers, obtained after hydrolysis of the poly[*tert*-butyl(meth)acrylate] block, are promising pH- and thermo-responsive materials for various applications related to biotechnology and stabilization of dispersions.[57]

Acknowledgment. This work was supported by the European Union within MC RTN POLYAMPHI and by DFG within the ESF EUROCORES Program SONS. We express our gratitude to the reviewers for their constructive criticism on the mechanism we proposed in the first version of this manuscript. This helped to considerably improve the mechanism and make it self-consistent. We thank Sabine Wunder (SEC), Cornelia Rettig, Kerstin Matussek, Manuela Schumacher, and Denise Danz (MALDI) for their help. X.A. acknowledges financial support by the French Research Ministry and the French−Bavarian University Center. Kh.B. acknowledges an "Erasmus−Socrates" exchange grant from the European Union. Michael Lanzendörfer (deceased) is gratefully acknowledged for fruitful discussions.

Supporting Information Available: Table with results of *t*BA and *t*BMA polymerization with DPHLi/LiCl, SEC traces, and MALDI-ToF mass spectra of the poly[*tert*-butyl (meth)acrylate] precursors, and of the poly(*N*,*N*-diethylacrylamide)s synthesized using diphenylhexyl-Li/Et_3Al. Linear and first-order time-conversion plots for the polymerization of DEAAm initiated by a poly(*tert*-butyl acrylate)-Li macroinitiator; calculation of the fraction of activated monomer and complexed chain ends. This material is available free of charge via the Internet at http://pubs.acs.org.

References and Notes

(1) Park, T. G.; Hoffman, A. S. *J. Appl. Polym. Sci.* **1992**, *46*, 659−671.
(2) Liu, H. Y.; Zhu, X. X. *Polymer* **1999**, *40*, 6985−6990.
(3) Butler, K.; Thomas, P. R.; Tyler, G. J. *J. Polym. Sci.* **1960**, *48*, 357−366.
(4) Huang, S. S.; McGrath, J. E. *J. Appl. Polym. Sci.* **1981**, *26*, 2827−2839.
(5) Xie, X.; Hogen-Esch, T. E. *Macromolecules* **1996**, *29*, 1746−1752.
(6) Kobayashi, M.; Okuyama, S.; Ishizone, T.; Nakahama, S. *Macromolecules* **1999**, *32*, 6466−6477.
(7) Nakhmanovich, B. I.; Urman, Y. G.; Arest-Yakubovich, A. A. *Macromol. Chem. Phys.* **2001**, *202*, 1327−1330.
(8) Freitag, R.; Baltes, T.; Eggert, M. *J. Polym. Sci., Part A: Polym. Chem.* **1994**, *32*, 3019−3030.
(9) Eggert, M.; Freitag, R. *J. Polym. Sci., Part A: Polym. Chem.* **1994**, *32*, 803−813.
(10) Kobayashi, M.; Ishizone, T.; Nakahama, S. *J. Polym. Sci., Part A: Polym. Chem.* **2000**, *38*, 4677−4685.
(11) Kobayashi, M.; Ishizone, T.; Nakahama, S. *Macromolecules* **2000**, *33*, 4411−4416.
(12) Ishizone, T.; Yoshimura, K.; Hirao, A.; Nakahama, S. *Macromolecules* **1998**, *31*, 8706−8712.
(13) Ishizone, T.; Yoshimura, K.; Yanase, E.; Nakahama, S. *Macromolecules* **1999**, *32*, 955−957.
(14) Kitayama, T.; Katsukawa, K.-i. *Polym. Bull.* **2004**, *52*, 117−124.
(15) Ute, K.; Nishimura, T.; Hatada, K. *Polym. J.* **1989**, *21*, 1027−1041.
(16) Haddleton, D. M.; Muir, A. V. G.; O'Donnell, J. P.; Richards, S. N.; Twose, D. L. *Macromol. Symp.* **1995**, *91*, 93−105.
(17) Uchiumi, N.; Hamada, K.; Kato, M.; Ono, T.; Yaginuma, S.; Ishiura, K. (Kuraray Co., Ltd.) EP 945470, 1999.
(18) Ballard, D. G. H.; Bowles, R. J.; Haddleton, D. M.; Richards, S. N.; Sellens, R.; Twose, D. L. *Macromolecules* **1992**, *25*, 5907−5913.
(19) Hirano, T.; Kitayama, T.; Cao, J.; Hatada, K. *Polym. J.* **2000**, *32*, 961−969.
(20) Kitayama, T.; Tabuchi, M.; Hatada, K. *Polym. J.* **2000**, *32*, 796−802.
(21) Hamada, K.; Shachi, K.; Ono, T.; Ishiura, K.; Takahashi, A. (Kuraray Co., Ltd.) JP 2002088109, 2002.
(22) Schlaad, H.; Schmitt, B.; Müller, A. H. E.; Jüngling, S.; Weiss, H. *Macromolecules* **1998**, *31*, 573−577.
(23) Schmitt, B.; Schlaad, H.; Müller, A. H. E. *Macromolecules* **1998**, *31*, 1705−1709.
(24) Schmitt, B.; Schlaad, H.; Müller, A. H. E.; Mathiasch, B.; Steiger, S.; Weiss, H. *Macromolecules* **2000**, *33*, 2887−2893.
(25) Baskaran, D.; Müller, A. H. E.; Sivaram, S. *Macromol. Chem. Phys.* **2000**, *201*, 1901−1911.
(26) Marchal, J.; Gnanou, Y.; Fontanille, M. *Makromol. Chem., Macromol. Symp.* **1996**, *107*, 27.
(27) Anderson, B. C.; Andrews, G. D.; Arthur, P., Jr.; Jacobson, H. W.; Melby, L. R.; Playtis, A. J.; Sharkey, W. H. *Macromolecules* **1981**, *14*, 1599.
(28) Schlaad, H.; Müller, A. H. E. *Macromolecules* **1998**, *31*, 7127−7132.
(29) Ihara, E.; Ikeda, J.-i.; Inoue, K. *Macromolecules* **2002**, *35*, 4223−4225.
(30) Ihara, E.; Ikeda, J.; Itoh, T.; Inoue, K. *Macromolecules* **2004**, *37*, 4048−4054.
(31) Ishizone, T.; Ito, M. *J. Polym. Sci., Part A: Polym. Chem.* **2002**, *40*, 4328−4332.
(32) Kitayama, T.; Shibuya, W.; Katsukawa, K.-I. *Polym. J.* **2002**, *34*, 405−409.
(33) Donovan, M. S.; Sanford, T. A.; Lowe, A. B.; Sumerlin, B. S.; Mitsukami, Y.; McCormick, C. L. *Macromolecules* **2002**, *35*, 4570−4572.
(34) Donovan, M. S.; Lowe, A. B.; Sumerlin, B. S.; McCormick, C. L. *Macromolecules* **2002**, *35*, 4123−4132.
(35) Schilli, C.; Lanzendörfer, M. G.; Müller, A. H. E. *Macromolecules* **2002**, *35*, 6819−6827.
(36) Teodorescu, M.; Matyjaszewski, K. *Macromolecules* **1999**, *32*, 4826−4831.
(37) Kizhakkedathu, J. N.; Kumar, K. R.; Goodman, D.; Brooks, D. E. *Polymer* **2004**, *45*, 7471−7489.
(38) Schierholz, K.; Givehchi, M.; Fabre, P.; Nallet, F.; Papon, E.; Guerret, O.; Gnanou, Y. *Macromolecules* **2003**, *36*, 5995−5999.
(39) Diaz, T.; Fischer, A.; Jonquieres, A.; Brembilla, A.; Lochon, P. *Macromolecules* **2003**, *36*, 2235−2241.
(40) Ray, B.; Isobe, Y.; Morioka, K.; Habaue, S.; Okamoto, Y.; Kamigaito, M.; Sawamoto, M. *Macromolecules* **2003**, *36*, 543−545.
(41) Ray, B.; Isobe, Y.; Matsumoto, K.; Habaue, S.; Okamoto, Y.; Kamigaito, M.; Sawamoto, M. *Macromolecules* **2004**, *37*, 1702−1710.

(42) Lutz, J.-F.; Neugebauer, D.; Matyjaszewski, K. *J. Am. Chem. Soc.* **2003**, *125*, 6986−6993.
(43) André, X.; Benmohamed, K.; Yakimansky, A. V.; Müller, A. H. E. *Proceedings of the 40th IUPAC International Symposium on Macromolecules*; Paris, France, 2004.
(44) Yakimansky, A. V.; Müller, A. H. E. Submitted to *Macromolecules*.
(45) Weiss, H.; Yakimanski, A. V.; Müller, A. H. E. *J. Am. Chem. Soc.* **1996**, *118*, 8897−8903.
(46) Lochmann, L.; Lim, D. *J. Organomet. Chem.* **1973**, *50*, 9−16.
(47) Long, T. E.; Liu, H. Y.; Schell, B. A.; Teegarden, D. M.; Uerz, D. S. *Macromolecules* **1993**, *26*, 6237−6242.
(48) Schmitt, B.; Stauf, W.; Müller, A. H. E. *Macromolecules* **2001**, *34*, 1551−1557.
(49) Schlaad, H.; Müller, A. H. E. *Macromol. Symp.* **1996**, *107*, 163−176.
(50) Yang, H. J.; Cole, C.-A.; Monji, N.; Hoffman, A. S. *J. Polym. Sci., Part A: Polym. Chem.* **1990**, *28*, 219−226.
(51) Ganachaud, F.; Monteiro, M. J.; Gilbert, R. G.; Dourges, M.-A.; Thang, S. H.; Rizzardo, E. *Macromolecules* **2000**, *33*, 6738−6745.
(52) Schilli, C.; Lanzendoerfer, M. G.; Mueller, A. H. E. *Macromolecules* **2002**, *35*, 6819−6827.
(53) Da, J.; Hogen-Esch, T. E. *J. Polym. Sci., Part A: Polym. Chem.* **2003**, *42*, 360−373.
(54) Montaudo, G., Montaudo, M. S., Samperi, F. *Mass Spectrometry of Polymers*; CRC Press: Boca Raton, London, New York, Washington DC, 2002.
(55) Litvinenko, G. I.; André, X.; Müller, A. H. E. **2005**, in preparation.
(56) Fayt, R.; Forte, R.; Jacobs, C.; Jérôme, R.; Ouhadi, T.; Teyssie, P.; Varshney, S. K. *Macromolecules* **1987**, *20*, 1442−1444.
(57) André, X.; Zhang, M.; Müller, A. H. E. *Macromol. Rapid Commun.* **2005**, *26*, 558−563.
(58) Kunkel, D. Ph.D. Thesis, Johannes-Gutenberg Universität, Mainz, Germany, 1992.
(59) Schmitt, B.; Müller, A. H. E. *Macromolecules* **2001**, *34*, 2115−2120.
(60) Janata, M.; Lochmann, L.; Mueller, A. H. E. *Makromol. Chem.* **1990**, *191*, 2253−2260.
(61) Janata, M.; Lochmann, L.; Vlcek, P.; Dybal, J.; Müller, A. H. E. *Makromol. Chem.* **1992**, *193*, 101−112.
(62) Zagala, A. P.; Dimov, D.; Hogen-Esch, T. E. *Macromol. Symp.* **1998**, *132*, 309−336.
(63) Aida, T.; Kuroki, M.; Sugimoto, H.; Watanabe, T.; Adachi, T.; Kawamura, C.; Inoue, S. *Makromol. Chem., Macromol. Symp.* **1993**, *67*, 125−135.
(64) Schlaad, H.; Müller, A. H. E. *Macromol. Symp.* **1995**, *95*, 13−26.
(65) Kunkel, D.; Müller, A. H. E.; Janata, M.; Lochmann, L. *Makromol. Chem., Macromol. Symp.* **1992**, *60*, 315−326.
(66) Kunkel, D.; Müller, A. H. E.; Janata, M.; Lochmann, L. *Polym. Prepr. (Am. Chem. Soc., Div. Polym. Chem.)* **1991**, *32*, 301−302.
(67) Gia, H.; McGrath, J. E. *Polym. Bull.* **1980**, *2*, 837−840.
(68) Huang, S. S.; McGrath, J. E. *Polym. Prepr. (Am. Chem. Soc., Div. Polym. Chem.)* **1983**, *24*, 138−140.
(69) Nakhmanovich, B. I.; Urman, Y. G.; Krystal'nyi, E. V.; Arest-Yakubovich, A. A. *Vysokomol. Soedin., Ser. A Ser. B* **2003**, *45*, 978−981.
(70) Martinez-Castro, N.; Zhang, M.; Pergushov, D. V.; Müller, A. H. E. *Des. Monomers Polym.* **2006**, *9*, 63−79.

MA051506A